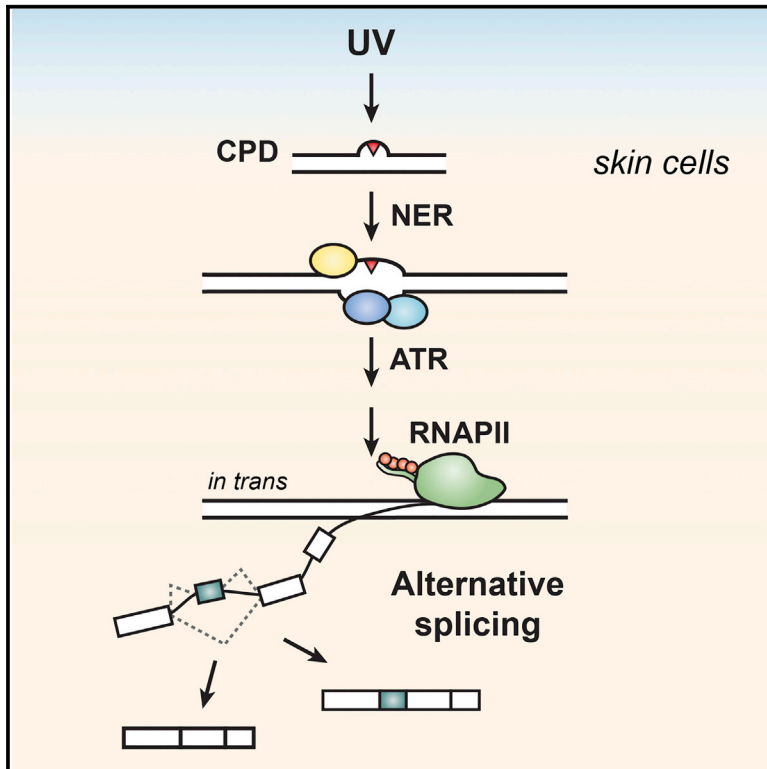


## Major Roles for Pyrimidine Dimers, Nucleotide Excision Repair, and ATR in the Alternative Splicing Response to UV Irradiation

### Graphical Abstract



### Authors

Manuel J. Muñoz, Nicolás Nieto Moreno, Luciana E. Giono, ..., Manuel Irimia, Marco Foiani, Alberto R. Kornblihtt

### Correspondence

ark@fbmc.fcen.uba.ar

### In Brief

Muñoz et al. find that UV-induced DNA damage is the main determinant affecting gene expression in response to UV in skin cells. DNA repair and the subsequent activation of ATR modulate RNAPII phosphorylation and alternative splicing patterns specifically in keratinocytes.

### Highlights

- DNA damage is sufficient to trigger a global alternative splicing (AS) response to UV
- Photolyase-mediated elimination of the DNA lesions (CPDs) abolishes the AS response
- RNAPII is the target, but not a sensor, of the signaling cascade initiated by CPDs
- GG-NER and ATR participate in the control of RNAPII phosphorylation and AS by UV

### Accession Numbers

GSE85510



# Major Roles for Pyrimidine Dimers, Nucleotide Excision Repair, and ATR in the Alternative Splicing Response to UV Irradiation

Manuel J. Muñoz,<sup>1,2,7</sup> Nicolás Nieto Moreno,<sup>1,7</sup> Luciana E. Giono,<sup>1,7</sup> Adrián E. Cambindo Botto,<sup>1</sup> Gwendal Dujardin,<sup>1,3,4</sup> Giulia Bastianello,<sup>2</sup> Stefania Lavore,<sup>2</sup> Antonio Torres-Méndez,<sup>3,4</sup> Carlos F.M. Menck,<sup>5</sup> Benjamin J. Blencowe,<sup>6</sup> Manuel Irimia,<sup>3,4</sup> Marco Foiani,<sup>2</sup> and Alberto R. Kornblihtt<sup>1,8,\*</sup>

<sup>1</sup>Instituto de Fisiología, Biología Molecular y Neurociencias (IFIBYNE-UBA-CONICET) and Departamento de Fisiología, Biología Molecular y Celular, Facultad de Ciencias Exactas y Naturales, Universidad de Buenos Aires, Ciudad Universitaria, C1428EHA Buenos Aires, Argentina

<sup>2</sup>Fondazione Istituto FIRC di Oncologia Molecolare (IFOM), Via Adamello 16, 20139 Milan, Italy

<sup>3</sup>Centre for Genomic Regulation, Barcelona Institute of Science and Technology (BIST), Dr. Aiguader 88, 08003 Barcelona, Spain

<sup>4</sup>Universitat Pompeu Fabra (UPF), 08003 Barcelona, Spain

<sup>5</sup>Departamento de Microbiologia, Instituto de Ciências Biomédicas, Universidade de São Paulo, São Paulo 05508-900, Brazil

<sup>6</sup>Donnelly Centre and Department of Molecular Genetics, University of Toronto, Toronto, ON M5S 3E1, Canada

<sup>7</sup>Co-first author

<sup>8</sup>Lead Contact

\*Correspondence: [ark@fbmc.fcen.uba.ar](mailto:ark@fbmc.fcen.uba.ar)

<http://dx.doi.org/10.1016/j.celrep.2017.02.066>

## SUMMARY

We have previously found that UV irradiation promotes RNA polymerase II (RNAPII) hyperphosphorylation and subsequent changes in alternative splicing (AS). We show now that UV-induced DNA damage is not only necessary but sufficient to trigger the AS response and that photolyase-mediated removal of the most abundant class of pyrimidine dimers (PDs) abrogates the global response to UV. We demonstrate that, in keratinocytes, RNAPII is the target, but not a sensor, of the signaling cascade initiated by PDs. The UV effect is enhanced by inhibition of gap-filling DNA synthesis, the last step in the nucleotide excision repair pathway (NER), and reduced by the absence of XPE, the main NER sensor of PDs. The mechanism involves activation of the protein kinase ATR that mediates the UV-induced RNAPII hyperphosphorylation. Our results define the sequence UV-PDs-NER-ATR-RNAPII-AS as a pathway linking DNA damage repair to the control of both RNAPII phosphorylation and AS regulation.

## INTRODUCTION

As a first barrier between the body interior and the exterior, our skin is regularly exposed to UV radiation. The UV light that reaches the Earth's surface can damage cellular components, such as DNA, RNA, proteins, and lipids, and is, therefore, the most prominent and ubiquitous carcinogen in our natural environment (Melnikova and Ananthaswamy, 2005). Despite the high incidence of skin cancer in human health and the fact that gene expression is a key target of signaling cascades triggered

by UV exposure, little is known about gene expression mechanisms occurring in response to UV light.

Alternative splicing (AS) is the main process that amplifies DNA information by generating multiple mRNA and protein variants from each of the vast majority (95%) of mammalian genes (Barash et al., 2010; Kornblihtt et al., 2013). AS has been shown to be regulated by external cues through various mechanisms whose alterations cause hereditary disease and cancer (Hua et al., 2011; Srebrow and Kornblihtt, 2006). This, together with findings of important biological roles for tissue- and species-specific AS patterns (Ellis et al., 2012; Gracheva et al., 2011), places the regulation of AS at the same level of importance as the regulation of transcription in the determination of cell differentiation and fate. We have previously identified transcriptional regulation and AS as crucial targets of signaling cascades resulting from UV irradiation of human cells. We have shown that UVC irradiation (<280 nm) promotes the phosphorylation of the C-terminal domain (CTD) of RNAPII, which slows down transcriptional elongation and affects AS of several genes, some of which are key for survival/apoptosis decisions (Muñoz et al., 2009). These observations were confirmed and extended by other genome-wide studies (Ip et al., 2011), which reinforced the evidence for physiological roles of the kinetic coupling between transcription and splicing. In this context, it is now known that, for alternative cassette exons, slow elongation can promote either exon inclusion (de la Mata et al., 2003; Muñoz et al., 2009) or skipping (Dujardin et al., 2014; Fong et al., 2014), depending on the regulatory *cis*-acting sequences and *trans*-acting factors operating in each particular AS event. Given the multiple cellular components susceptible to be damaged by UV light, it was important to evaluate whether damage of DNA or of other cell molecules trigger the AS response. The most conspicuous UV-induced DNA lesions are cyclobutane pyrimidine dimers (CPDs) and 6-4 pyrimidine-pyrimidone photoproducts ((6-4)PPs), both of which are, at least in placental mammals, mainly repaired by the nucleotide excision

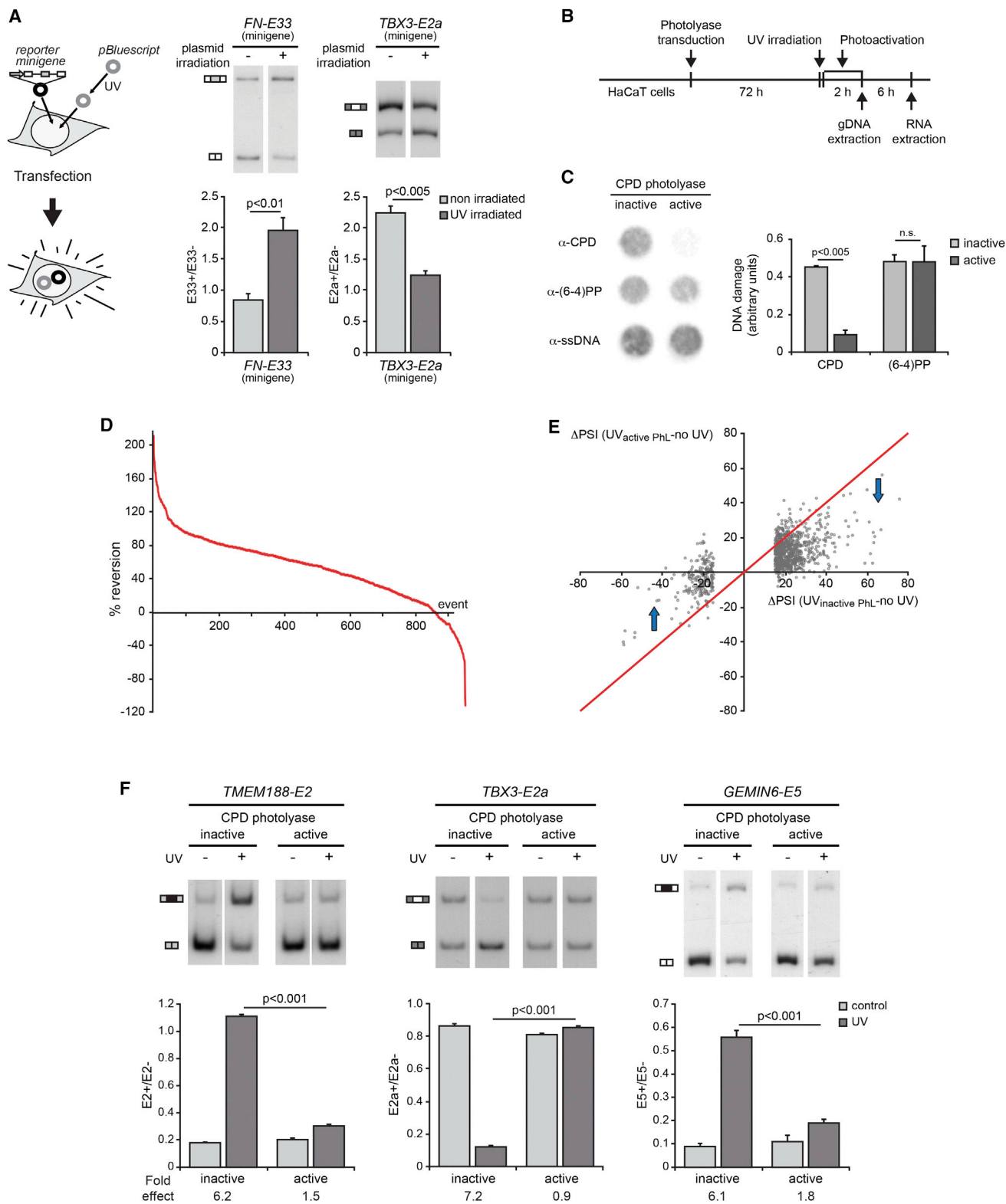


**Figure 1. Cyclobutane Pyrimidine Dimers Are Responsible for the UV Effect on AS in Skin Cells**

(A) HaCaT cells were co-transfected with pBluescript (pBS) or pBS irradiated in vitro with  $1,500 \text{ J/m}^2$  UV together with *FN-E33* or *TBX3-E2a* reporter minigenes for 24 hr. AS patterns of *FN* or *TBX3* were assessed by radioactive RT-PCR with specific primers for the minigenes-derived mRNAs. The ratio inclusion/skipping is shown.

(legend continued on next page)

repair (NER) system (Marteijn et al., 2014). NER is initiated by two distinct DNA-damage-sensing mechanisms that use the same machinery to repair the damage: transcription coupled repair (TCR or TC-NER) and global genome repair (GGR or GG-NER). TC-NER detects and removes damage from the template strand of genes that are being transcribed and depends on RNAPII elongation and on the Cockayne syndrome proteins CSA and CSB. Mutations in this pathway are associated with cell death probably due to deficiencies in transcriptional re-start after damage (Anindya et al., 2010). GG-NER, the repair mechanism that prevails in keratinocytes, the most abundant cell type in the skin (D'Errico et al., 2007), removes UV-induced damage present in both transcribed and non-transcribed regions of the genome and depends on the UV-DDB complex, in which XPE interacts with the lesion, and on XPC to detect the damage. Once the damage is recognized by either TC-NER or GG-NER factors, both pathways converge at the recruitment of the general transcription factor TFIIH, which opens the DNA helix around the damage. After the recruitment of XPA and the endonucleases XPF and XPG to excise the damaged strand, the resulting single-stranded DNA (ssDNA) gap is filled by DNA synthesis and ligation (Marteijn et al., 2014).

DNA damage not only induces DNA repair but triggers signaling pathways as well. Ataxia telangiectasia mutated (ATM) and ataxia telangiectasia mutated and Rad3 related (ATR), members of the PI(3)-like protein kinase family, are enzymes of paramount importance in the DNA damage response. Whereas ATR was originally identified as a key factor controlling DNA replication in S phase, it was later shown to be activated throughout the cell cycle by ssDNA generated during NER (Hanasoge and Ljungman, 2007; Marteijn et al., 2009; Matsu-moto et al., 2007; Stiff et al., 2008; Vrouwe et al., 2011). Moreover, it was also shown that ATR activation by UV irradiation in turn activates ATM (Stiff et al., 2006).

Here, we provide direct proof that UV-induced CPDs are sufficient to initiate the AS response in skin cells without the involvement of any other type of UV-damaged molecules. Photolyase-mediated removal of CPDs abolished the UV-induced RNAPII phosphorylation and AS regulation, therefore demonstrating that CPDs are the main trigger in the modulation of two key steps of gene expression in UV-treated keratinocytes. Transfection experiments with irradiated plasmids that serve as templates for transcription suggest that RNAPII is a target,

but not a sensor, of the DNA lesion. Our results reveal that ATR acts as a bridging signal from the DNA lesion to the RNAPII phosphorylation/AS regulation in a NER-dependent manner.

## RESULTS

### Cyclobutane Pyrimidine Dimers Are Responsible for the UV Effect on RNAPII Phosphorylation and AS in Skin Cells

We have previously found that, in hepatoma cells, UV irradiation regulates co-transcriptional AS in a p53-independent manner, through the phosphorylation of RNAPII CTD and subsequent inhibition of transcriptional elongation (Muñoz et al., 2009). In order to determine whether damage of DNA, and not of other types of cell components, was sufficient to trigger RNAPII hyperphosphorylation and AS regulation in human keratinocytes (HaCaT cells), we used two different approaches: (1) transfection of UV-damaged naked plasmid DNA without irradiation of cells and (2) irradiation of cells followed by prompt removal of DNA lesions. In the first strategy, to avoid the concomitant damage of RNA, proteins, lipids, and other molecules after UV treatment of cells, a water solution of a plasmid with no relevant sequences for mammalian cells, pBluescript (pBS), was irradiated in vitro with UV light and co-transfected with two different AS reporter model minigenes: one carrying an alternative exon whose inclusion is upregulated by UV irradiation (*FN-E33*) and another with an alternative exon whose skipping is promoted (*TBX3-E2a*). Co-transfection of the minigenes with the in-vitro-irradiated pBS caused an increase in *FN-E33* inclusion and in *TBX3-E2a* skipping in the absence of cell irradiation, mimicking the UV effect (Figure 1A). It is important to point out that the in-vitro-irradiated plasmid preserved its circular integrity and that, as expected for the effects of UV irradiation, did not contain double-strand breaks (Figure S1A).

These experiments indicate that damaged DNA is sufficient to trigger a splicing response that is independent of the potential effects of damaging other cell molecules. It also confirmed, using a different experimental approach, our previous demonstration that the UV effect on AS is not a consequence of DNA damage in cis, i.e., on the actual template DNA encoding the alternative mRNA isoforms (Muñoz et al., 2009), but rather of a systemic or global cell response to damage. In the second approach, we reasoned that, if damaged DNA is the cause of AS modulation

(B) Diagram showing the adenovirus infection protocol. Immediately following UV irradiation, the photolyase was activated by treatment with white light for 2 hr. Genomic DNA (gDNA) and RNA were extracted at the indicated time points.

(C) Repair of DNA lesions in HaCaT cells transduced with the CPD photolyase as described in (B) was assessed by DNA western dot blot using specific antibodies against CPD, 6-4(PP), or total single-stranded DNA (ssDNA).

(D) HaCaT cells transduced with CPD photolyase-expressing adenovirus were left untreated (no UV) or UV irradiated. Irradiated cells were then exposed to white light to activate the photolyase (UV, active PhL) or kept in the dark (UV, inactive PhL). Global transcriptome analysis was performed to compare irradiated cells with an active or inactive CPD photolyase. y axis, percentage of reversion of UV-induced changes for alternatively spliced cassette exons following photolyase photoactivation. Positive percent values represent reversion of UV-induced AS changes toward control levels.

(E) Reversion of changes in inclusion levels induced by UV by expression of photolyase. The x axis represents the  $\Delta$ PSI of each event between UV, inactive PhL and no UV samples, using a 15% threshold. The y axis shows the values of  $\Delta$ PSI for the same events in respect to the control when the photolyase is active (UV, active PhL). The red line represents the relation between the  $\Delta$ PSI of UV, inactive PhL minus control with respect of the  $\Delta$ PSI of UV, active PhL minus control, i.e., the absence of photolyase effect on UV-induced changes. The blue arrows indicate the direction of the changes where reversion is happening.

(F) AS patterns in CPD photolyase-transduced HaCaT cells treated with 15 J/m<sup>2</sup> UV were assessed 6 hr after photolyase activation by radioactive RT-PCR.

For all experiments, images of a representative experiment and mean, SEM, and p values (Student's t test) of three experiments are shown. See also Figures S1 and S2 and Tables S1 and S2.

upon UV irradiation, then treatment of cells with UV light followed by removal of DNA lesions should not produce AS changes. As mentioned earlier, the most abundant UV-induced DNA pyrimidine dimer (PD) lesions are CPDs. This type of lesion induces little distortion in the double helix and consequently is poorly repaired by the NER pathway (Garcin et al., 2007), the main system dealing with UV-induced DNA damage in humans. How can we dissociate UV treatment and formation of CPDs if these are slowly repaired but heavily induced by UV light? Photolyases are white-light-activated flavoenzymes that specifically revert the different lesions generated by UV irradiation. The fact that placental mammals do not possess photolyases offers an invaluable opportunity to use a CPD-specific photolyase from a marsupial mammal (*Potorous tridactylus*, the Australian rat kangaroo) as a tool to selectively abolish the contribution of CPDs. HaCaT cells were transduced with an adenovirus expressing the *Potorous* CPD photolyase and, 72 hr later, treated with 15 J/m<sup>2</sup> of UV. The photolyase was then activated by exposing the cells to white light for 2 hr or keeping them in the dark as a control, after which cells were harvested (Figure 1B). After total DNA purification, damage was assessed by DNA western dot blot using antibodies specific to CPD, (6-4)PP, or to ssDNA as control. Figure 1C shows that photolyase activation reduced the amount of CPDs by about 80%, keeping the levels of (6-4)PPs unaffected. Similar results were obtained by immunostaining of fixed cells with the same antibodies (Figure S1B).

In order to assess the global effects of UV irradiation on AS and the extent of the CPD contribution to these effects, we performed RNA sequencing (RNA-seq) analysis of duplicate samples of photolyase-transduced HaCaT cells, left untreated (“no UV”), UV irradiated and kept in the dark (“UV, inactive PhL”), or UV irradiated and photoactivated for 2 hr with white light (“UV, active PhL”). We analyzed the variations in the percentage of alternative exon inclusion (PSI [percent spliced in]) for each AS event (ASE) that were greater than 15% ( $\Delta\text{PSI} > 15\%$ ; see [Experimental Procedures](#)). We observed that irradiation with 15 J/m<sup>2</sup> of UV light altered the inclusion levels of 1,551 ASEs (UV, inactive PhL versus no UV; Figure S1C). These events occurred in 1,174 unique genes, indicating that UV affects the splicing pattern of a considerable proportion of genes expressed in HaCaT cells (~11% of the total number of multiexonic genes expressed in these samples). Approximately 64% (991) of the affected ASEs are cassette exons, in which we focused our analysis. Of these, 77.8% (771) show higher inclusion upon UV treatment. We found that removal of CPDs by photoactivation of the marsupial photolyase reverted the effects of UV light to different extents in the majority (87%) of the cassette exon events (Figure 1D), with 56% of the affected exons reverting their PSI at least by 50%.

To study the contribution of CPDs in more detail, we compared the  $\Delta\text{PSI}$  between the UV-irradiated and control samples (UV, inactive PhL versus no UV) with their corresponding  $\Delta\text{PSI}$  in samples from cells with active photolyase with respect to control (UV, active PhL versus no UV; Figure 1E). Each dot corresponds to one of the 991 alternative exons whose inclusion changes upon UV irradiation. Strikingly, most cassette exons with either higher or lower inclusion levels upon UV treatment (x axis) show a clear reduction in the  $\Delta\text{PSI}$  caused by UV when the photolyase is active (y axis), observed by a general displace-

ment from the diagonal toward the horizontal axis (blue arrows). In the type of graphic shown in Figure 1E, if the photolyase activity had no effect, all dots would be aligned along the diagonal. These results strongly indicate that CPDs are the main cause of the AS response to UV light.

Figures 1F and S1D show the validation of the RNA-seq data (Table S1) by individual RT-PCR analysis of seven endogenous ASEs, which include the *TBX3-E2a* example used in Figure 1A. Consistent with results in Figure 1A, the change in AS observed in the *FN-E33* exon is also reverted by the photolyase (Figure S1E).

To study a putative contribution of (6-4)PPs in the cellular response to UV, we conducted a similar set of experiments using the specific (6-4)PP photolyase from *Arabidopsis thaliana* (Figures S2A–S2C). Figure S2C shows that, unlike CPDs, complete removal of (6-4)PPs does not alter the UV effect on AS. This may reflect the fact that CPDs are induced roughly five times more than (6-4)PPs (Besaratina et al., 2011) when using, as we do, a UVC lamp with an emission peak of 254 nm. Yet, the most harmful UV radiation that reaches the Earth’s surface is not UVC but UVB (305 nm), because UV radiation below 305 nm is filtered by the ozone layer (Besaratina et al., 2011). We then compared the effect on AS and RNAPII phosphorylation of UVC and UVB. For both wavelengths (254 and 305 nm), we used doses that generated comparable amounts of CPDs but different amounts of (6-4)PPs (Figure S2D). Under these conditions, we found that UV-induced RNAPII phosphorylation, shown as RNAPII<sub>o</sub>/RNAPII<sub>a</sub> ratio (Figure S2E), and AS patterns (Figure S2F) were affected at comparable levels in UVC- or UVB-treated cells, further strengthening the role of CPDs in the response to UV light and suggesting that UVB acts in a similar fashion as UVC.

Although the importance of the effect of CPDs on gene expression has been addressed before (Boros et al., 2015), the crosstalk between CPD’s impact in mRNA levels and AS has not been documented. We found that activation of the CPD photolyase, but not the (6-4)PP photolyase, prevented the UV-induced increase in the RNAPII<sub>o</sub>/RNAPII<sub>a</sub> ratio (Figures 2A and S3A), as well as both up- and downregulation of gene expression levels (Figure 2B). Moreover, the ASEs affected by UV in both directions (increased and decreased PSI) often correspond to genes whose expression is downregulated by UV (Figure 2C), and most importantly, photolyase-triggered reversion of AS changes clearly takes place in genes whose expression is downregulated by UV (Figure 2D), consistently with a role for a reduction in RNAPII elongation. In agreement with this, phosphomimetic CTD mutants and a slow elongation RNAPII mutant duplicate the UV effect on AS in skin cells, whereas non-phosphorylatable mutants prevent the UV effect (Figures S3B and S3C), confirming previous results from our group obtained in a different cell line (Muñoz et al., 2009). Therefore, results in Figure 2 suggest that the effect of CPDs on AS is mediated by RNAPII, which could act either as a sensor of damage or as an effector of signaling cascades triggered by CPDs.

### The AS Response to UV Is Not Triggered by an Active RNAPII nor by Transcription-Coupled Repair

It has been recently proposed that, in human fibroblasts, RNAPII stalling in UV-damaged genes modulates AS through

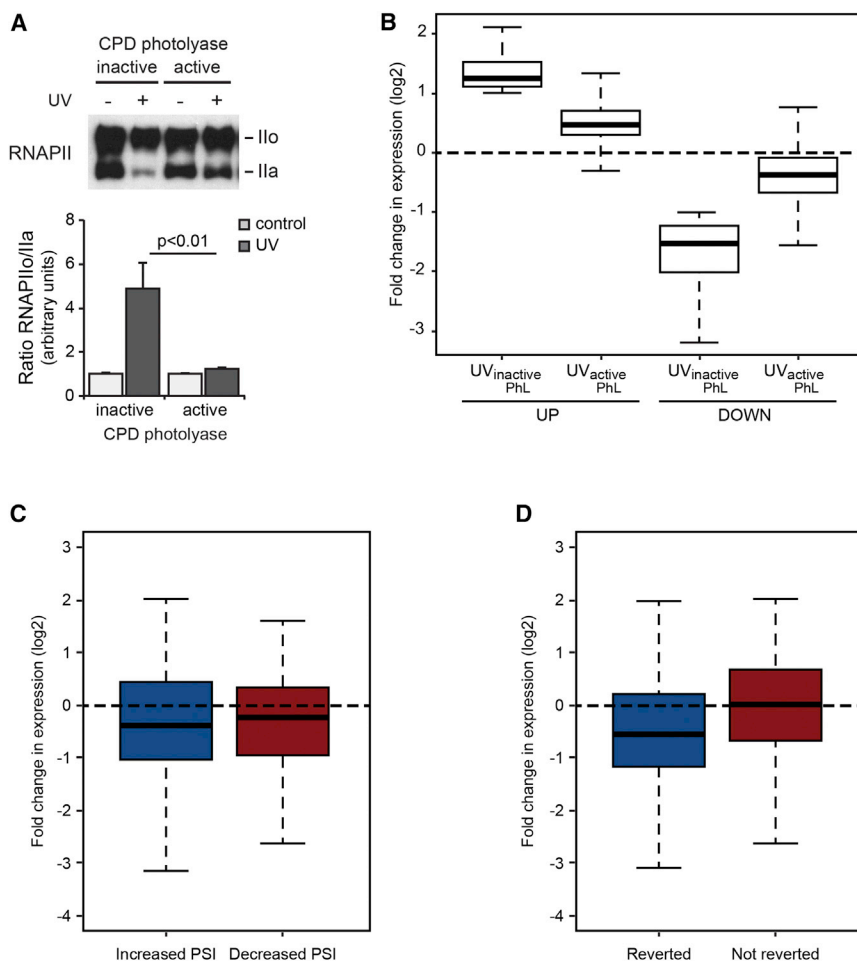


**Figure 2. Cyclobutane Pyrimidine Dimers Modulate RNAPII Phosphorylation and Gene Expression Levels**

(A) RNAPII phosphorylation status in CPD photolyase-transduced HaCaT cells treated with 15 J/m<sup>2</sup> UV was assessed 2 hr after photolyase activation. Global RNAPII phosphorylation pattern was determined by western blot using an antibody against the N-terminal part of RNAPII major subunit (Rbp1) and quantification of the phospho RNAPII (Ilo) to non-phospho RNAPII (Ila) ratio. Images of a representative experiment and mean, SEM, and p values (Student's t test) of two experiments are shown.

(B) Global transcriptome analysis of CPD photolyase-transduced HaCaT cells. Reversion of UV-induced changes in gene expression following photolyase photoactivation (UV, active PhL versus UV, inactive PhL) for genes increasing or decreasing their expression levels by at least 2-fold up and down, respectively.

(C) Distribution of changes in steady-state levels upon UV treatment for genes that contain cassette exons with increased (blue) or decreased (red) inclusion. For clarity, outliers are not plotted.

(D) Distribution of changes in steady-state levels for genes whose AS cassette exons are dependent on CPDs (reverted by photolyase expression by at least 50%) or not.

See also [Figure S3](#).

an R-loop-dependent mechanism (Tresini et al., 2015). Results in [Figure 1A](#) suggest that, at least in keratinocytes, this is not the case because the pBS plasmid irradiated in vitro, which is effective in triggering the AS response, does not carry an RNAPII promoter. To further evaluate the potential role of an active RNAPII as a sensor of the CPD effect on AS, we replaced the pBS plasmid with a luciferase reporter vector with (pGL3-SV40; Promega pGL3-Control) or without (pGL3; Promega pGL3-Basic) the strong RNAPII promoter of the SV40 virus. [Figure 3A](#) shows that the presence of the SV40 promoter allows for transcription of the pGL3 plasmid, revealed by the elicited luciferase activity (compare bars 1 and 3). Although UV irradiation reduces transcription, irradiated pGL3-SV40 still displays about 5,000 times more luciferase activity than irradiated pGL3 (compare bars 2 and 4). Despite the qualitative difference in transcription capabilities, the in-vitro-irradiated pGL3 and pGL3-SV40 plasmids elicited similar effects on *FN-E33* and *TBX3-E2a* minigenes AS patterns ([Figure 3B](#)), indicating that transcription of the irradiated plasmid is not required for the AS response to damaged DNA. This evidence points to a lack of roles for RNAPII as a lesion sensor and therefore of the involvement of TC-NER in the AS response in keratinocytes. To confirm these predictions, we first investigated whether TC-NER is involved in the AS response to

protein depletion of approximately 80% ([Figures S4A and S4B](#)). Similar results were obtained when irradiating patient-derived CSB mutant cells or a control counterpart stably expressing a wild-type version of CSB ([Figure S4C](#)).

To understand our results obtained in keratinocytes in the context of the observations made in fibroblasts (Tresini et al., 2015), we compared the UV response in both cell types. Results in [Figure 3D](#) show that fibroblasts and keratinocytes behave differently upon UV irradiation: whereas UV promotes inclusion of the *FN-E33* in keratinocytes, it induces skipping in fibroblasts. We then analyzed the effects of co-transfecting the *FN-E33* AS reporter minigene together with in-vitro-irradiated pGL3 or pGL3-SV40 in fibroblasts and found that the need for transcription of the irradiated plasmid to elicit the respective AS responses differs between the two cell types. Whereas in keratinocytes, the presence or absence of an RNAPII promoter in the pGL3 vector is dispensable to mimic the UV effect ([Figure 3B](#)), in fibroblasts, there is a clear need for transcription of the irradiated plasmid to duplicate the UV effect ([Figure 3E](#)).

These experiments independently indicate that, although RNAPII seems to be an important target of the signaling elicited by CPD lesions ([Figure 2A](#)), the enzyme is not acting as the main sensor for the CPD effect on AS in human keratinocytes,

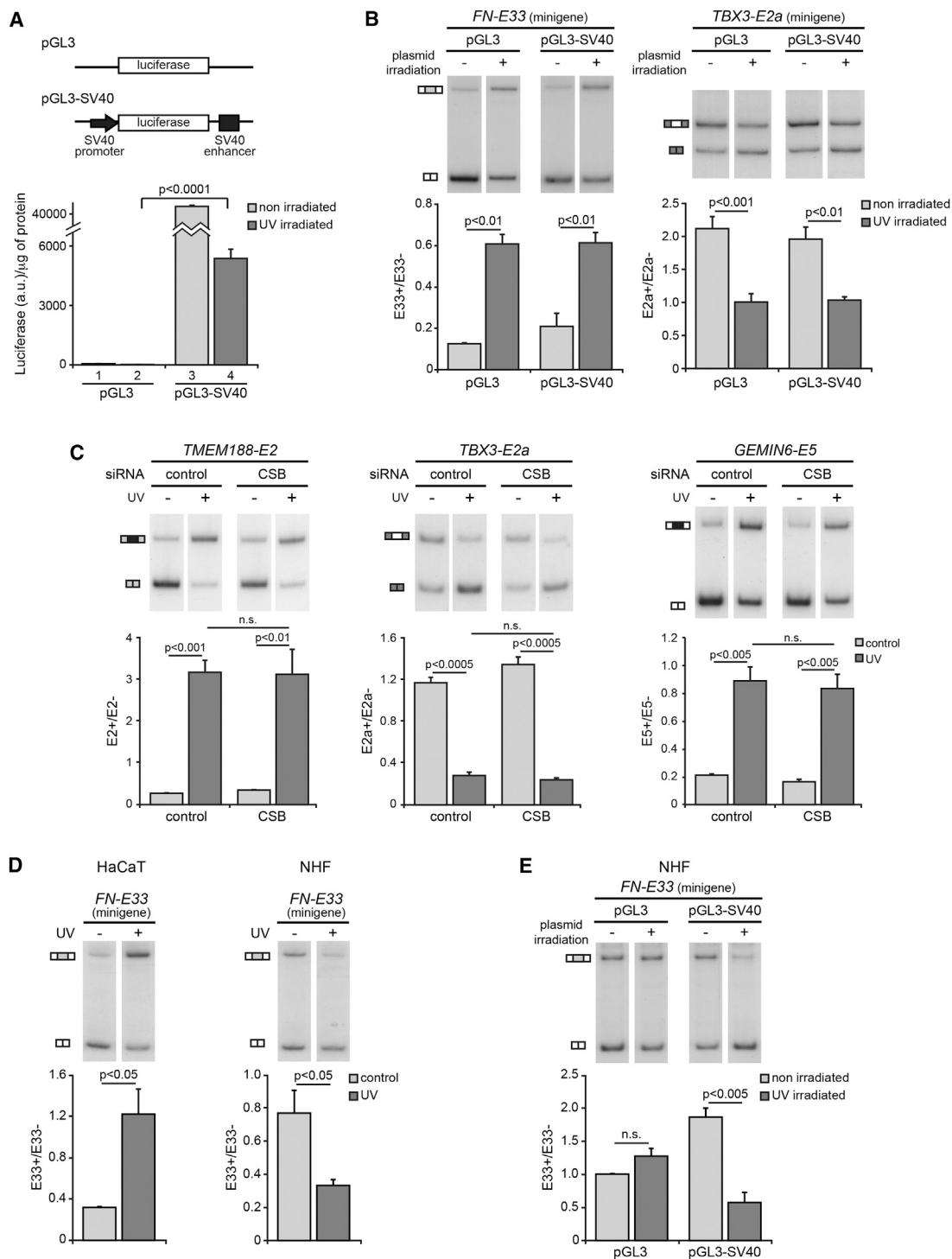


**Figure 3. AS Regulation by UV Is Not Triggered by RNAPII nor TC-NER**

(A) Expression of the luciferase reporter plasmids pGL3 basic (pGL3) or pGL3 control (pGL3-SV40) for untreated or in-vitro-irradiated vectors 24 hr after transfection.

(B) HaCaT cells were co-transfected with pGL3 or pGL3-SV40 vectors, either untreated or in vitro irradiated, together with *FN-E33* or *TBX3-E2a* minigene reporters for 24 hr. AS patterns of *FN* or *TBX3* were assessed as in Figure 1A.

(C) HaCaT cells were transfected with 25 nM of control or CSB siRNA oligonucleotides for 72 hr. Cells were irradiated with 15 J/m<sup>2</sup> UV, and AS of the indicated endogenous genes was assayed as described in Figure 1.

(legend continued on next page)

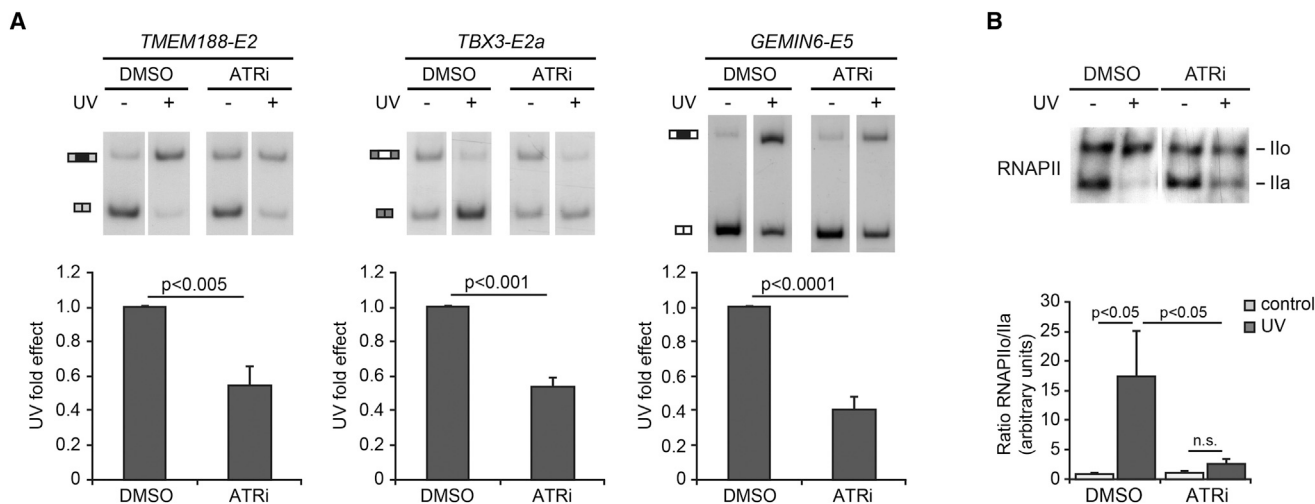


**Figure 4. ATR Modulates AS Patterns and RNAPII Phosphorylation in Response to UV Light**

(A) HaCaT cells were pre-treated with 10  $\mu$ M ATR inhibitor ETP-46464 (ATRi) 1 hr prior to UV irradiation (15 J/m<sup>2</sup>). After 6 hr, AS of the indicated endogenous genes was assayed as described.

(B) RNAPII phosphorylation status (phospho RNAPII [Ilo] to non-phospho RNAPII [Ila] ratio) in HaCaT cells pre-treated with ATRi was analyzed 2 hr after UV irradiation with 15 J/m<sup>2</sup>. Images of a representative experiment and mean, SEM, and p values (Student's t test) of three experiments are shown.

See also Figure S5.

in contrast to what has been reported by Tresini and co-workers in fibroblasts. Taken together, these results demonstrate the differences in the mechanisms controlling gene expression in different cell types and highlight the importance of using the most appropriate model when analyzing the effects of a natural carcinogen as UV light.

We then investigated the involvement of other systems capable of interacting with DNA lesions, such as DNA replication. To evaluate the role of an active DNA polymerase as a sensor of damaged DNA, we sorted control and UV-treated HaCaT cells, based on their DNA content, to analyze AS patterns in G1, S, and G2/M populations. The UV effect proved to be of comparable magnitude in all cell cycle phases (Figure S4D), with no particular increase in S phase, which suggests that the replisome is not a main sensor for the UV effect on AS.

Finally, and having in mind that GG-NER, but not TC-NER, is the main system in charge of DNA repair in keratinocytes (D'Errico et al., 2007), we reasoned that a reduced CPD recognition would elicit a reduced UV effect on AS. Using CRISPR-Cas9 technology, we found that ablation of XPE, the main factor in charge of CPD recognition, partially decreased the UV effect on AS (Figures S4E and S4F), strongly suggesting a role for DNA repair in the control of gene expression in skin cells.

Results so far suggest that, in keratinocytes, where GG-NER prevails, XPE, but not RNAPII, acts as one of the lesion sensors for the AS response.

### ATR Modulates the Alternative Splicing Response to CPDs

In view of results in Figure 3, given that the UV effect is of comparable magnitude in G1, S, and G2/M (Figure S4D), the fact that NER is active throughout the cell cycle (Sancar et al., 2004) and the decreased UV effect on AS in XPE-null cells (Figure S4F), we thought that the repair system itself could be responsible for damage sensing and signaling. A key event that follows NER is the activation of ATR (Hanasoge and Ljungman, 2007; Marteinj et al., 2009; Matsumoto et al., 2007; Stiff et al., 2008; Vrouwe et al., 2011), which, in turn, can activate ATM (Stiff et al., 2006). To investigate the contribution of these kinases in the AS response to CPDs, we irradiated HaCaT cells pre-treated with ATR or ATM inhibitors, whose specificities were verified by their abilities to inhibit Chk1 or Chk2 phosphorylation, respectively (Figure S5A). For the three ASEs used as models, ATR inhibition reduced the UV effect on AS patterns (Figure 4A) by at least 50%. A less pronounced inhibition was observed when inhibiting ATM (Figure S5B). We then analyzed the roles of ATR and ATM in the UV-induced RNAPII hyperphosphorylation. Figure 4B shows that the increase in RNAPII<sub>o</sub>/RNAPII<sub>a</sub> ratio caused by UV is prevented by the ATR inhibitor. Such a strong role for ATR in the phosphorylation of the CTD is unprecedented and likely indirect, considering that, to date, the main Ser/Thr kinases shown to directly phosphorylate the CTD are CDK7, CDK9, CDK12, and CDK13 (Barkowiak et al., 2010; Muñoz et al., 2010). The actual

(D) HaCaT cells or normal human fibroblasts (NHF) were transfected with the *FN-E33* reporter minigene. After 4 hr, cells were UV irradiated (15 J/m<sup>2</sup>) and harvested 24 hr later. AS patterns of *FN* were assessed by radioactive RT-PCR with specific pairs of primers for the minigene-derived mRNAs.

(E) Normal human fibroblasts were co-transfected with pGL3 or pGL3-SV40 vectors, either untreated or in vitro irradiated, together with the *FN-E33* minigene reporter for 24 hr. AS patterns of *FN* were assessed as described.

For all experiments, images of a representative experiment and mean, SEM, and p values (Student's t test) of three experiments are shown. See also Figure S4.

target(s) of ATR remain yet to be identified. Similar to what happened with AS regulation, ATM inhibition impaired the UV-induced hyperphosphorylation of RNAPII but to a much lesser extent (Figure S5C).

### NER Links CPD Repair to ATR Activation and the AS Response in Keratinocytes

It has been shown that ATR activation is triggered by ssDNA segments generated after incision by NER nucleases to remove the damaged strand and before the participation of DNA polymerases to copy the undamaged strand (Marteijn et al., 2014). Figure 5A shows that photolyase-dependent removal of CPDs inhibits the UV-induced ATR activation, indicated by the increase in the phosphorylation levels of Chk1. To further evaluate the role of the NER pathway on ATR activation in conditions in which general DNA replication does not occur, we first obtained non-cycling HaCaT cells through a serum deprivation protocol reported by the Sancar group (Kemp and Sancar, 2016; Figure S5D). As shown in Figure 5B (compare lanes 1 and 2), UV irradiation of non-cycling HaCaT cells activates ATR as indicated by Chk1 phosphorylation. Moreover, this activation also takes place in the presence of actinomycin D, a general inhibitor of transcription (lanes 3 and 4; Figure S5E), thus favoring the idea that ATR can be activated in response to UV but in the absence of both replication and transcriptional stress. More interestingly, and in agreement with published evidence that UV-induced photolesions elicit ATR kinase-dependent signaling in non-cycling cells (Vrouwe et al., 2011), inhibition of repair synthesis by aphidicolin resulted in ATR over-activation (Figure 5C). More importantly, aphidicolin treatment greatly enhanced the UV effect on AS (Figure 5D) and increased the RNAPII<sub>o</sub>/RNAPII<sub>a</sub> ratio (Figure 5E). Unlike previous experiments where UV irradiation was performed at 15 J/m<sup>2</sup>, here we used a lower dose (5 J/m<sup>2</sup>) in order to better visualize the enhancement of all three processes by aphidicolin. We propose that prevention of gap-filling to replace the damaged strand keeps ssDNA segments exposed, which then activates ATR, causing in turn changes in AS via RNAPII phosphorylation.

### DISCUSSION

DNA, RNA, proteins, and lipids, as well as many other molecules within the cell, can function as UV light receptors, as they absorb UV radiation and produce signals in response to it. Whereas the global consequences of skin exposure to sunlight are clear, ranging from inflammation, erythema, or photoaging to skin cancer, the molecular pathways triggering such responses are only partially understood.

In the present work, we show that, upon UV irradiation, DNA damage is not only necessary but sufficient to modulate AS in human keratinocytes. By transfecting in-vitro-damaged plasmid DNA, we have recapitulated the UV effect on AS. It is worth noting that, unlike plasmid DNA, transfection of irradiated small double-stranded oligo-deoxynucleotides (20 mers) into HaCaT cells had no effect on AS (data not shown). We attribute this failure to the reported evidence that short double-stranded DNA is not a good substrate for NER (Kulaksiz et al., 2005; Shell et al., 2013), the pathway we report here as responsible for the effects

of UV light on AS. Our results rule out roles for RNA, protein, or lipid damage in the AS response. This does not imply that RNA damage, for example, is exempt from playing other roles, like the reported stimulation of the production of the inflammatory cytokines tumor necrosis factor  $\alpha$  (TNF- $\alpha$ ) and interleukin-6 (IL-6) (Bernard et al., 2012), which in turn modulate gene expression patterns in a skin system.

Using a photoactivable marsupial photolyase in placental mammalian (human) skin cells, we demonstrate that the AS and RNAPII responses are triggered by the CPD photoproducts generated upon UV irradiation. According to their functional category or gene ontology terms, the RNA-seq analysis revealed more than 170 genes whose AS patterns are affected by UV and reverted by the CPD photolyase by at least 50% are involved in apoptosis, cell cycle, or DNA damage (Table S2). This confirms the functional relevance of the AS response to UV, studied in more depth in our previous report (Muñoz et al., 2009). The photolyase also reverted RNAPII CTD hyperphosphorylation (Figure 2A), strengthening our previous evidence that this event mediates the change in AS. On the contrary, under the experimental conditions used in this work, we did not observe changes in RNAPII phospho status, nor in the AS events analyzed herein, when expressing the (6-4)PP photolyase. A possible explanation is that CPDs are heavily induced, whereas (6-4)PPs are only mildly formed, upon UV irradiation. In any case, we cannot rule out a role for (6-4)PPs in the AS response to UV light.

RNA-seq analysis showed that CPDs are the main cause of the UV effect on AS because 87% of the ASEs affected by UV showed total or partial reversion with the photolyase. UV treatment increased inclusion of 78% and skipping of 22% of cassette exons, the prevalent modality of AS in mammalian keratinocytes (Figure S1C). Abrogation of CPDs by the photolyase reverts both types of changes but, most importantly, when gene expression and AS analyses are combined, it becomes clear that UV regulation of both “up” and “down” cassette exons (Figure 2C) and photolyase reversion (Figure 2D) occur in genes whose expression is reduced by UV. We interpret this as an indicator that CPDs are acting through the modulation of RNAPII elongation rates because most reversions occur when there are changes in expression levels.

Three different experiments support the conclusion that, in contrast to what was reported for fibroblasts (Tresini et al., 2015), in keratinocytes, the cell type normally exposed to sunlight, RNAPII is the target, but not the sensor, of the UV effect. First, the effects of in-vitro-damaged plasmid DNA on AS were identical whether the plasmid sequences were being transcribed or not (Figure 3B). Second, in this case, in agreement with evidence provided by Tresini et al. (2015), depletion of the TC-NER factor CSB had no influence on the AS response to UV irradiation (Figures 3C and S4C). Third, and unlike to what happened in keratinocytes, the use of an in-vitro-irradiated plasmid carrying a strong RNAPII promoter, but not the same vector without the promoter, mimicked the UV effect on AS in fibroblasts (Figure 3E), confirming the role of RNAPII as a sensor of damage in this cell type. This experiment highlights differences in the mechanism controlling gene expression between keratinocytes, the most common cell type naturally affected

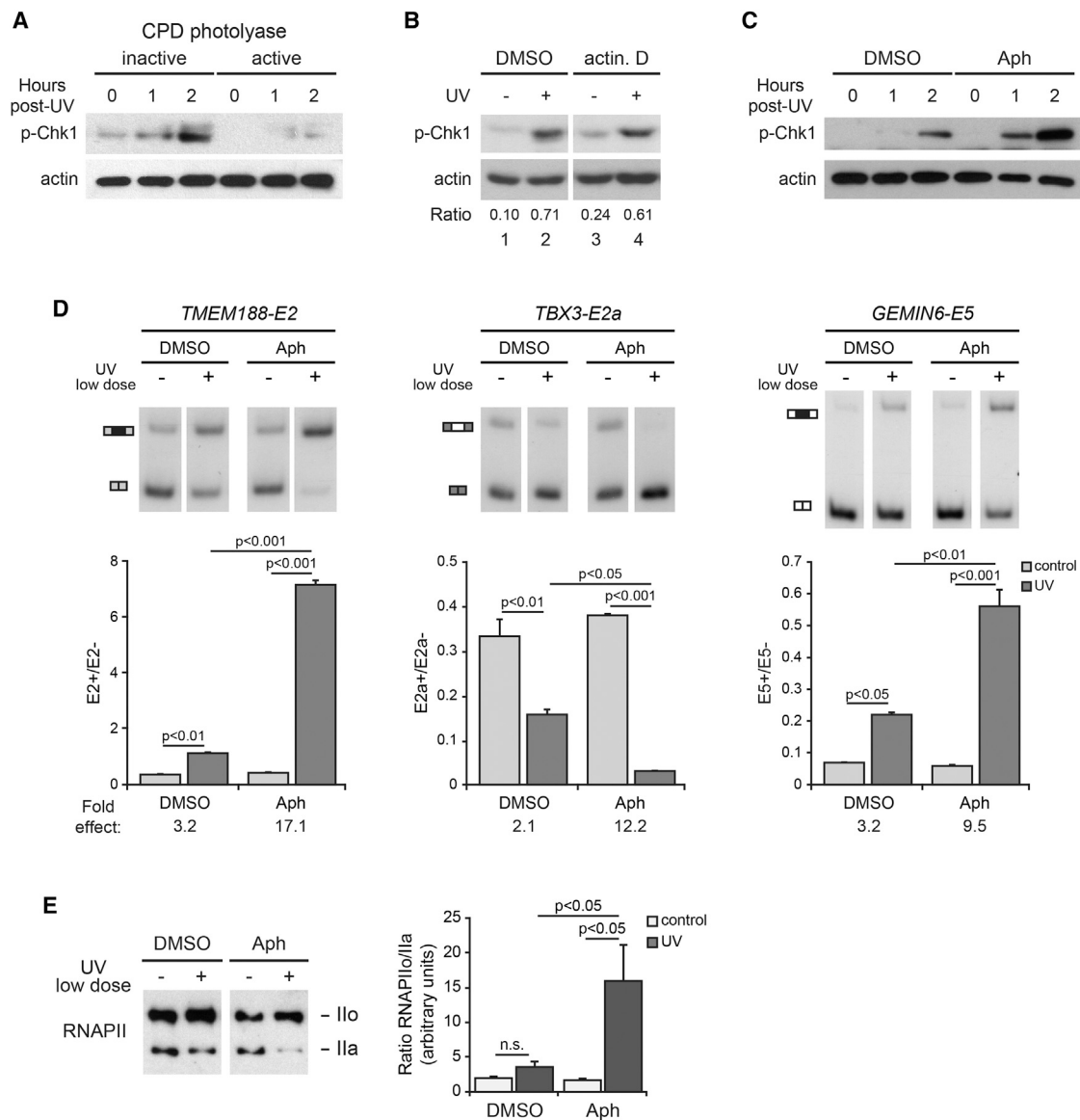


**Figure 5. Inhibition of DNA Gap-Filling Enhances the UV-Induced RNAPII Hyperphosphorylation and AS Regulation**

(A) Levels of phosphorylated Chk1 (Ser317) were analyzed in CPD photolyase-transduced HaCaT cells at the indicated times after UV irradiation (15 J/m<sup>2</sup>) followed by 1 hr of photolyase photoactivation.

(B) Non-cycling HaCaT cells were pre-treated with 5 ng/μL actinomycin D (actin. D) for 4 hr prior to UV irradiation (15 J/m<sup>2</sup>). Two hours later, the levels of phosphorylated Chk1 (Ser317) were analyzed by western blot. Numbers represent the p-Chk1 to actin ratio.

(C–E) Non-cycling HaCaT cells were treated with 5 μg/mL aphidicolin (Aph) for 1 hr prior to low UV dose irradiation (5 J/m<sup>2</sup>). (C) Two hours later, the levels of phosphorylated Chk1 (Ser317) were analyzed by western blot. (D) AS patterns of the indicated endogenous genes were determined as described. Mean, SEM, and p values of a representative experiment are shown. (E) Two hours after UV treatment, the phospho RNAPII (Ilo) to non-phospho RNAPII (Ila) ratio was determined by western blot. Images of a representative experiment and mean, SEM, and p values (Student's t test) of two experiments are shown. See also Figure S5.

by sunlight, and fibroblasts. We would like to point out that many experiments in the published literature were performed using patient-derived fibroblasts with defects in repair mechanisms (TC-NER, GG-NER, etc.). In view of results in this work, some of the observations derived from fibroblasts-based experiments would need revision when drawing conclusions about the effects of UV light in the skin.

A lack of role for TC-NER in our cell system coincides with evidence that GG-NER prevails in keratinocytes (D'Errico et al., 2005, 2007; Mouret et al., 2008). In any case, both mechanisms repair CPDs throughout the cell cycle and involve the generation of ssDNA, which was shown to activate the PI(3)-like kinase ATR (Hanasoge and Ljungman, 2007; Marteiijn et al., 2009; Matsu-moto et al., 2007; Stiff et al., 2008; Vrouwe et al., 2011). Using

a specific inhibitor, we show here that ATR participates in the CPD signaling both at the levels of RNAPII phosphorylation (Figure 4B) and AS (Figure 4A). In agreement with these results, and using the photolyase strategy, we showed that CPDs lead to activation of the ATR protein kinase (Figure 5A) independently of replication or transcriptional stress (Figure 5B). Because CPD repair by NER generates ssDNA intermediates that activate ATR, we focused on the inhibition of the last step in NER and found that inhibition of the gap-filling DNA synthesis by aphidicolin increased the UV effect on AS, RNAPII phosphorylation, and ATR activation (Figures 5C–5E).

We believe that ATR promotes RNAPII CTD phosphorylation indirectly because there are no recognizable ATR target sequences in the CTD. We cannot rule out effects of ATR at the level of phosphorylation of other proteins, apart from RNAPII, such as splicing factors (Matsuoka et al., 2007). These results unveil a new role for ATR in the control of gene expression at the transcription and splicing levels, with the signaling cascade UV-PD-ATR-RNAPII-AS as the most likely scenario. Moreover, if ATR activation by any means was similar, then the effect in S phase (in which ATR can be activated not only by NER but also by a stalled DNA polymerase) should be different than the effect in G1 or G2/M. Because results in Figure S4D showed that the UV effect on AS was similar in all cell cycles phases, we speculate that different modes of ATR activation, i.e., replication dependent or independent, would activate ATR in a different way, thus affecting different substrates or pathways. In any case, more research is needed to deeply understand the modes and consequences of ATR activation.

Tresini et al. (2015) reported that UV modulates AS in fibroblasts through an RNAPII and R-loop-dependent mechanism that activates ATM. In our keratinocyte model, we observed that ATM modulates RNAPII phosphorylation and AS (Figures S5B and S5C) but to a lesser extent than ATR. Despite this, it is unlikely that the role of ATM in the control of AS in keratinocytes can be explained by the mechanism proposed by Tresini et al. Results in Figure 3 demonstrate not only that RNAPII is not the lesion sensor but also that the mechanisms acting in fibroblasts and keratinocytes to modulate gene expression in a genotoxic scenario are different. A possible explanation for ATM's participation is its crosstalk with ATR, as it has been shown that, upon UV, ATR can activate ATM (Stiff et al., 2006). Finally, and in good agreement with the above-proposed mechanism, we found that ablation of GG-NER and CPD recognition factor XPE decreased the UV effect on AS. In view of this, it is tempting to speculate that repair-deficient cells from xeroderma pigmentosum patients would exhibit gene expression defects.

In summary, we described a pathway connecting UV-induced DNA lesions and their repair to ATR activation. This work highlights the importance of ATR in the control of gene expression programs in a genotoxic scenario throughout the cell cycle.

## EXPERIMENTAL PROCEDURES

### Cell Culture and Treatments

HaCaT cells and normal human fibroblasts (NHF) were cultured as indicated by ATCC. For experiments performed with non-cycling cells, HaCaT cells were grown to confluence and further incubated for 3 days in low serum (0.5% fetal

bovine serum [FBS]) medium as described (Kemp and Sancar, 2016). When indicated, cells were pre-incubated for 1 hr before UV irradiation with the following drugs: ATR inhibitor 10  $\mu$ M (ETP-46464; CNIO); aphidicolin 5  $\mu$ g/mL (Sigma); or for 4 hr with actinomycin D 5 ng/ $\mu$ L (Sigma).

### UV Irradiation

Cells were washed once with PBS prior to UVC (254 nm) irradiation. UV irradiation was performed with a CL-1000 Shortwave Crosslinker (UVP) with an emission peak at 254 nm. The doses were quantified by its internal sensor. Unless otherwise indicated, the UV dose was 15 J/m<sup>2</sup> whereas low UV dose was 5 J/m<sup>2</sup>. For in vitro irradiation of plasmids, drops of no more than 20  $\mu$ L were deposited on Parafilm and irradiated with 1,500 J/m<sup>2</sup> of UV.

### DNA Western Dot Blot

Cells were harvested and total DNA was extracted with QIAmp DNA Mini Kit (QIAGEN) according to the manufacturer's protocol. DNA was quantified, denatured, and equal amounts were blotted on a nitrocellulose Hybond N+ membrane (GE Healthcare). DNA western dot blot was performed according to Perdiz et al. (2000), with minor changes. To assess the amount of CPDs, (6-4)PPs, and ssDNA, membranes were incubated with appropriate dilutions of anti-CPD or anti-(6-4)PP antibodies (TDM-2 and 64M-2; Cosmo Bio) and anti-ssDNA (MAB3034; Millipore). Signal was detected using the LI-COR Biosciences Odyssey Imager with the appropriate secondary antibodies and quantified with the ImageStudio software (LI-COR Biosciences).

### Transfections

Transfection of siRNAs and AS reporter minigenes was performed using Lipofectamine 2000 (Thermo Scientific) according to manufacturer's instructions and as described in Muñoz et al. (2009). siRNAs were purchased from GE-Dharmacon: SMARTpool siGENOME ERCC6 (CSB; cat. no. M-004888) and siNegative-Control no. 2 (cat. no. D-001206-14).

### AS Reporter Minigenes

*FN-E33* reporter minigene was previously described (de la Mata and Kornblihtt, 2006). *TBX3-E2a* minigene was obtained by cloning a DNA fragment containing the alternative exon E2a, its flanking introns, and part of the upstream and downstream exons into the BstEII sites of the pUHC-CFTR minigene (Dujardin et al., 2014). The *FN-E33* and *TBX3-E2a* reporter minigenes were co-transfected with a plasmid expressing the tetracycline-controlled transactivator (tTA)-VP16. Transcription of the minigenes was allowed by removal of tetracycline following UV irradiation.

### RNA Extraction and Radioactive RT-PCR Analysis

RNA was purified using TriPure reagent (Roche Life Science). Conditions and primers for radioactive RT-PCR of endogenous or reporter minigenes are described in the Supplemental Experimental Procedures.

### Adenoviral Photolyase Transduction and Photoactivation

HaCaT cells plated on 12-well dishes were transduced with adenoviruses expressing the CPD photolyase from *Potorous tridactylus* or the (6-4)PP photolyase from *Arabidopsis thaliana* (de Lima-Bessa et al., 2008) at a MOI of 15,000 in 260  $\mu$ L of DMEM with 2% FBS. After 2 hr, 0.5 mL of growth medium were added and cells were additionally incubated for 72 hr. The expression of the photolyases was indirectly monitored by examining EGFP expression through fluorescence microscopy. For photoactivation, cells were washed with PBS, UV irradiated, and covered with 0.5 mL of DMEM without phenol red, with 10% FBS. Dishes were placed on a 4-mm-thick glass placed above a fluorescent lamp (GE FCL 22W/D Daylight 22W 12K). Companion dishes were wrapped in aluminum foil and treated similarly.

### Global Transcriptomic Analysis of Alternative Splicing

HaCaT cells transduced with CPD photolyase-expressing adenovirus were left untreated (no UV) or UV irradiated. Irradiated cells were then exposed to white light to activate the photolyase (UV, active PhL) or kept in the dark (UV, inactive PhL). Cells were harvested 6 hr after photoactivation, and total RNA was extracted from two biological replicates of each condition, prepared using

the Illumina TruSeq mRNA kit, and sequenced on an Illumina HiSeq2000. For details, see [Supplemental Experimental Procedures](#).

### Luciferase Assay

Cells were transfected with 250 ng of pGL3 vectors (Promega). Twenty-four hours after transfection, luciferase activity was measured using the Luciferase Reporter Assay System (Promega) according to the manufacturer's instructions.

### ACCESSION NUMBERS

The accession number for the RNA-seq data reported in this paper is GEO: GSE85510.

### SUPPLEMENTAL INFORMATION

Supplemental Information includes Supplemental Experimental Procedures, five figures, and two tables and can be found with this article online at <http://dx.doi.org/10.1016/j.celrep.2017.02.066>.

### AUTHOR CONTRIBUTIONS

M.J.M., L.E.G., and N.N.M. designed and performed most experiments. A.E.C.B., G.D., G.B., and S.L. performed some experiments. M.I., A.T.-M., and B.J.B. performed the bioinformatics analysis of the RNA-seq experiments. C.F.M.M. participated in the design of the photolyase experiments. M.F. critically read the manuscript and contributed with scientific advice. M.J.M. and A.R.K. wrote the manuscript and supervised the whole work.

### ACKNOWLEDGMENTS

We thank F. Coin, V. Gottfredi, and G. Soria for useful discussions and reagents as well as members of the lab, especially V. Buggiano and A. Srebrow, for their help and support. We also thank E. Cafferata for his invaluable help with the adenovirus purification and D. González Maglio for HaCaT cells. A.R.K. and M.J.M. received support from the Agencia Nacional de Promoción Científica y Tecnológica de Argentina (PICT-2011 1617, PICT-2014 2582), the Universidad de Buenos Aires (UBACYT 20020130100152BA), and the Alberto J. Roemmers Foundation. G.D. was supported by Marie Curie International Outgoing Fellowship within the EU Seventh Framework Programme for Research and Technological Development (FP7/2007-2013) under grant agreement 275632. B.J.B. is supported by grants from the Canadian Institutes of Health Research (FDN 148434). M.I. is supported by grants from the European Research Council (ERC-StG-LS2- 637591) and from Ministerio de Economía y Competitividad (BFU2014-55076-P; MINECO). A.T.-M. is supported by an FPI-SO fellowship from the Spanish Ministry of Economy and Competitiveness. M.F. is supported by the Associazione Italiana per la Ricerca sul Cancro (AIRC) and Telethon-Italy. G.B. is recipient of a fellowship from the University of Milan. S.L. is an employee of IFOM Cell Biology Unit. M.J.M., L.E.G., and A.R.K. are career investigators and N.N.M. and A.E.C.B. are recipients of a graduate student fellowship from the Consejo Nacional de Investigaciones Científicas y Técnicas de Argentina (CONICET). A.R.K. is a Senior International Research Scholar of the Howard Hughes Medical Institute.

Received: November 14, 2016

Revised: January 11, 2017

Accepted: February 21, 2017

Published: March 21, 2017

### REFERENCES

Anindya, R., Mari, P.-O., Kristensen, U., Kool, H., Giglia-Mari, G., Mullenders, L.H., Foustier, M., Vermeulen, W., Egly, J.-M., and Svejstrup, J.Q. (2010). A ubiquitin-binding domain in Cockayne syndrome B required for transcription-coupled nucleotide excision repair. *Mol. Cell* **38**, 637–648.

Barash, Y., Calarco, J.A., Gao, W., Pan, Q., Wang, X., Shai, O., Blencowe, B.J., and Frey, B.J. (2010). Deciphering the splicing code. *Nature* **465**, 53–59.

Bartkowiak, B., Liu, P., Phatnani, H.P., Fuda, N.J., Cooper, J.J., Price, D.H., Adelman, K., Lis, J.T., and Greenleaf, A.L. (2010). CDK12 is a transcription elongation-associated CTD kinase, the metazoan ortholog of yeast Ctk1. *Genes Dev.* **24**, 2303–2316.

Bernard, J.J., Cowing-Zitron, C., Nakatsuji, T., Muehleisen, B., Muto, J., Borowski, A.W., Martinez, L., Greidinger, E.L., Yu, B.D., and Gallo, R.L. (2012). Ultraviolet radiation damages self noncoding RNA and is detected by TLR3. *Nat. Med.* **18**, 1286–1290.

Besaratinia, A., Yoon, J.-I., Schroeder, C., Bradforth, S.E., Cockburn, M., and Pfeifer, G.P. (2011). Wavelength dependence of ultraviolet radiation-induced DNA damage as determined by laser irradiation suggests that cyclobutane pyrimidine dimers are the principal DNA lesions produced by terrestrial sunlight. *FASEB J.* **25**, 3079–3091.

Boros, G., Miko, E., Muramatsu, H., Weissman, D., Emri, E., van der Horst, G.T., Szegedi, A., Horkay, I., Emri, G., Karikó, K., and Remenyik, É. (2015). Identification of cyclobutane pyrimidine dimer-responsive genes using UVB-irradiated human keratinocytes transfected with in vitro-synthesized photolyase mRNA. *PLoS ONE* **10**, e0131141.

D'Errico, M., Teson, M., Calcagnile, A., Nardo, T., De Luca, N., Lazzari, C., Soddu, S., Zambruno, G., Stefanini, M., and Dogliotti, E. (2005). Differential role of transcription-coupled repair in UVB-induced response of human fibroblasts and keratinocytes. *Cancer Res.* **65**, 432–438.

D'Errico, M., Lemma, T., Calcagnile, A., Proietti De Santis, L., and Dogliotti, E. (2007). Cell type and DNA damage specific response of human skin cells to environmental agents. *Mutat. Res.* **614**, 37–47.

de la Mata, M., and Kornblihtt, A.R. (2006). RNA polymerase II C-terminal domain mediates regulation of alternative splicing by SRp20. *Nat. Struct. Mol. Biol.* **13**, 973–980.

de la Mata, M., Alonso, C.R., Kadener, S., Fededa, J.P., Blaustein, M., Pelisch, F., Cramer, P., Bentley, D., and Kornblihtt, A.R. (2003). A slow RNA polymerase II affects alternative splicing in vivo. *Mol. Cell* **12**, 525–532.

de Lima-Bessa, K.M., Armelini, M.G., Chiganças, V., Jacysyn, J.F., Amarante-Mendes, G.P., Sarasin, A., and Menck, C.F. (2008). CPDs and 6-4PPs play different roles in UV-induced cell death in normal and NER-deficient human cells. *DNA Repair (Amst.)* **7**, 303–312.

Dujardin, G., Lafaille, C., de la Mata, M., Marasco, L.E., Muñoz, M.J., Le Josic-Corcos, C., Corcos, L., and Kornblihtt, A.R. (2014). How slow RNA polymerase II elongation favors alternative exon skipping. *Mol. Cell* **54**, 683–690.

Ellis, J.D., Barrios-Rodiles, M., Colak, R., Irimia, M., Kim, T., Calarco, J.A., Wang, X., Pan, Q., O'Hanlon, D., Kim, P.M., et al. (2012). Tissue-specific alternative splicing remodels protein-protein interaction networks. *Mol. Cell* **46**, 884–892.

Fong, N., Kim, H., Zhou, Y., Ji, X., Qiu, J., Saldi, T., Diener, K., Jones, K., Fu, X.D., and Bentley, D.L. (2014). Pre-mRNA splicing is facilitated by an optimal RNA polymerase II elongation rate. *Genes Dev.* **28**, 2663–2676.

Garcin, G., Douki, T., Stoebner, P.E., Guesnet, J., Guezennec, A., Martinez, J., Cadet, J., and Meunier, L. (2007). Cell surface expression of melanocortin-1 receptor on HaCaT keratinocytes and alpha-melanocortin stimulation do not affect the formation and repair of UVB-induced DNA photoproducts. *Photochem. Photobiol. Sci.* **6**, 585–593.

Gracheva, E.O., Cordero-Morales, J.F., González-Carcacia, J.A., Ingolia, N.T., Manno, C., Aranguren, C.I., Weissman, J.S., and Julius, D. (2011). Ganglion-specific splicing of TRPV1 underlies infrared sensation in vampire bats. *Nature* **476**, 88–91.

Hanasoge, S., and Ljungman, M. (2007). H2AX phosphorylation after UV irradiation is triggered by DNA repair intermediates and is mediated by the ATR kinase. *Carcinogenesis* **28**, 2298–2304.

Hua, Y., Sahashi, K., Rigo, F., Hung, G., Horev, G., Bennett, C.F., and Krainer, A.R. (2011). Peripheral SMN restoration is essential for long-term rescue of a severe spinal muscular atrophy mouse model. *Nature* **478**, 123–126.

- Ip, J.Y., Schmidt, D., Pan, Q., Ramani, A.K., Fraser, A.G., Odom, D.T., and Blencowe, B.J. (2011). Global impact of RNA polymerase II elongation inhibition on alternative splicing regulation. *Genome Res.* *21*, 390–401.
- Kemp, M.G., and Sancar, A. (2016). ATR kinase inhibition protects non-cycling cells from the lethal effects of DNA damage and transcription stress. *J. Biol. Chem.* *291*, 9330–9342.
- Kornblihtt, A.R., Schor, I.E., Alló, M., Dujardin, G., Petrillo, E., and Muñoz, M.J. (2013). Alternative splicing: a pivotal step between eukaryotic transcription and translation. *Nat. Rev. Mol. Cell Biol.* *14*, 153–165.
- Kulaksiz, G., Reardon, J.T., and Sancar, A. (2005). Xeroderma pigmentosum complementation group E protein (XPE/DDB2): purification of various complexes of XPE and analyses of their damaged DNA binding and putative DNA repair properties. *Mol. Cell. Biol.* *25*, 9784–9792.
- Marteijn, J.A., Bekker-Jensen, S., Mailand, N., Lans, H., Schwertman, P., Gourdin, A.M., Dantuma, N.P., Lukas, J., and Vermeulen, W. (2009). Nucleotide excision repair-induced H2A ubiquitination is dependent on MDC1 and RNF8 and reveals a universal DNA damage response. *J. Cell Biol.* *186*, 835–847.
- Marteijn, J.A., Lans, H., Vermeulen, W., and Hoeijmakers, J.H. (2014). Understanding nucleotide excision repair and its roles in cancer and ageing. *Nat. Rev. Mol. Cell Biol.* *15*, 465–481.
- Matsumoto, M., Yaginuma, K., Igarashi, A., Imura, M., Hasegawa, M., Iwabuchi, K., Date, T., Mori, T., Ishizaki, K., Yamashita, K., et al. (2007). Perturbed gap-filling synthesis in nucleotide excision repair causes histone H2AX phosphorylation in human quiescent cells. *J. Cell Sci.* *120*, 1104–1112.
- Matsuoka, S., Ballif, B.A., Smogorzewska, A., McDonald, E.R., 3rd, Hurov, K.E., Luo, J., Bakalarski, C.E., Zhao, Z., Solimini, N., Lerenthal, Y., et al. (2007). ATM and ATR substrate analysis reveals extensive protein networks responsive to DNA damage. *Science* *316*, 1160–1166.
- Melnikova, V.O., and Ananthaswamy, H.N. (2005). Cellular and molecular events leading to the development of skin cancer. *Mutat. Res.* *571*, 91–106.
- Mouret, S., Charveron, M., Favier, A., Cadet, J., and Douki, T. (2008). Differential repair of UVB-induced cyclobutane pyrimidine dimers in cultured human skin cells and whole human skin. *DNA Repair (Amst.)* *7*, 704–712.
- Muñoz, M.J., Pérez Santangelo, M.S., Paronetto, M.P., de la Mata, M., Pelisch, F., Boireau, S., Glover-Cutter, K., Ben-Dov, C., Blaustein, M., Lozano, J.J., et al. (2009). DNA damage regulates alternative splicing through inhibition of RNA polymerase II elongation. *Cell* *137*, 708–720.
- Muñoz, M.J., de la Mata, M., and Kornblihtt, A.R. (2010). The carboxy terminal domain of RNA polymerase II and alternative splicing. *Trends Biochem. Sci.* *35*, 497–504.
- Perdiz, D., Grof, P., Mezzina, M., Nikaido, O., Moustacchi, E., and Sage, E. (2000). Distribution and repair of bipyrimidine photoproducts in solar UV-irradiated mammalian cells. Possible role of Dewar photoproducts in solar mutagenesis. *J. Biol. Chem.* *275*, 26732–26742.
- Sancar, A., Lindsey-Boltz, L.A., Unsal-Kaçmaz, K., and Linn, S. (2004). Molecular mechanisms of mammalian DNA repair and the DNA damage checkpoints. *Annu. Rev. Biochem.* *73*, 39–85.
- Shell, S.M., Hawkins, E.K., Tsai, M.S., Hlaing, A.S., Rizzo, C.J., and Chazin, W.J. (2013). Xeroderma pigmentosum complementation group C protein (XPC) serves as a general sensor of damaged DNA. *DNA Repair (Amst.)* *12*, 947–953.
- Srebrow, A., and Kornblihtt, A.R. (2006). The connection between splicing and cancer. *J. Cell Sci.* *119*, 2635–2641.
- Stiff, T., Cersaletti, K., Concannon, P., O'Driscoll, M., and Jeggo, P.A. (2008). Replication independent ATR signalling leads to G2/M arrest requiring Nbs1, 53BP1 and MDC1. *Hum. Mol. Genet.* *17*, 3247–3253.
- Stiff, T., Walker, S.A., Cersaletti, K., Goodarzi, A.A., Petermann, E., Concannon, P., O'Driscoll, M., and Jeggo, P.A. (2006). ATR-dependent phosphorylation and activation of ATM in response to UV treatment or replication fork stalling. *EMBO J.* *25*, 5775–5782.
- Tresini, M., Warmerdam, D.O., Kolovos, P., Snijder, L., Vrouwe, M.G., Demmers, J.A., van IJcken, W.F., Grosveld, F.G., Medema, R.H., Hoeijmakers, J.H., et al. (2015). The core spliceosome as target and effector of non-canonical ATM signalling. *Nature* *523*, 53–58.
- Vrouwe, M.G., Pines, A., Overmeer, R.M., Hanada, K., and Mullenders, L.H. (2011). UV-induced photolesions elicit ATR-kinase-dependent signaling in non-cycling cells through nucleotide excision repair-dependent and -independent pathways. *J. Cell Sci.* *124*, 435–446.

**Cell Reports, Volume 18**

## **Supplemental Information**

**Major Roles for Pyrimidine Dimers, Nucleotide**

**Excision Repair, and ATR in the Alternative**

**Splicing Response to UV Irradiation**

**Manuel J. Muñoz, Nicolás Nieto Moreno, Luciana E. Giono, Adrián E. Cambindo Botto, Gwendal Dujardin, Giulia Bastianello, Stefania Lavore, Antonio Torres-Méndez, Carlos F.M. Menck, Benjamin J. Blencowe, Manuel Irimia, Marco Foiani, and Alberto R. Kornblihtt**

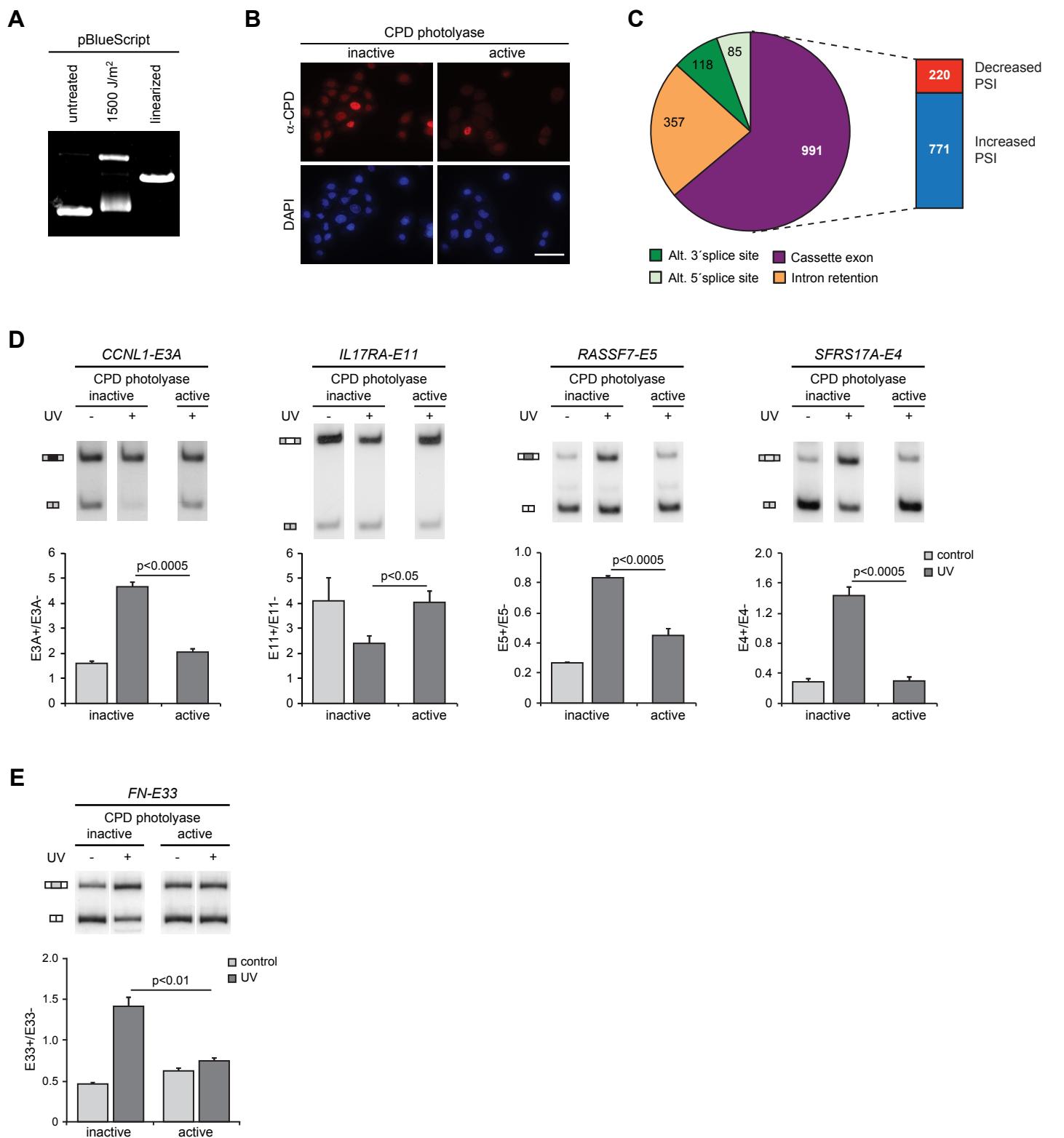


**Figure S1. Cyclobutane Pyrimidine Dimers Are Responsible for the UV Effect on AS, Related to Figure 1**

**(A)** Integrity of *in vitro*-irradiated pBlueScript. pBlueScript was *in vitro*-irradiated with 1500 J/m<sup>2</sup> or linearized with EcoRI. Topoisomers were resolved in a 1% agarose gel and stained with ethidium bromide after electrophoresis.

**(B)** CPD repair by *Potorous tridactylus* CPD photolyase. HaCaT cells plated on coverslips were transduced with an adenovirus expressing the CPD photolyase from *Potorous tridactylus*. After 72 h, cells were irradiated with 15 J/m<sup>2</sup> and the photolyase was activated by exposure to white light for 2 h. Immediately following photoreactivation, cells were fixed and CPD levels were detected by indirect immunofluorescence. Scale bar represents 20 μm.

**(C)** Global transcriptome analysis of AS changes in HaCaT cells treated with UV light. RNA from HaCaT cells treated or not with 15 J/m<sup>2</sup> of UV ("UV, inactive PhL" vs. "no UV") were subjected to RNA-Seq analysis. Number of AS events showing changes in inclusion levels (absolute average ΔPSI > 15 and a range PSI difference between samples of at least 5) upon UV treatment in HaCaT cells, plotted by class; right, for cassette exons, percent of exons that increase (blue) or decrease (red) inclusion upon UV treatment. PSI: Percent Spliced In.

**(D)** Validation of RNA-Seq events. CPD-photolyase transduced HaCaT cells were irradiated with 15 J/m<sup>2</sup> of UV and harvested 6 h after photolyase activation. AS of the indicated endogenous genes was assessed by radioactive RT-PCR.

**(E)** CPD-photolyase transduced HaCaT cells were irradiated with 15 J/m<sup>2</sup> of UV and, 24 h after photolyase activation, AS of *FN* was assessed by radioactive RT-PCR.

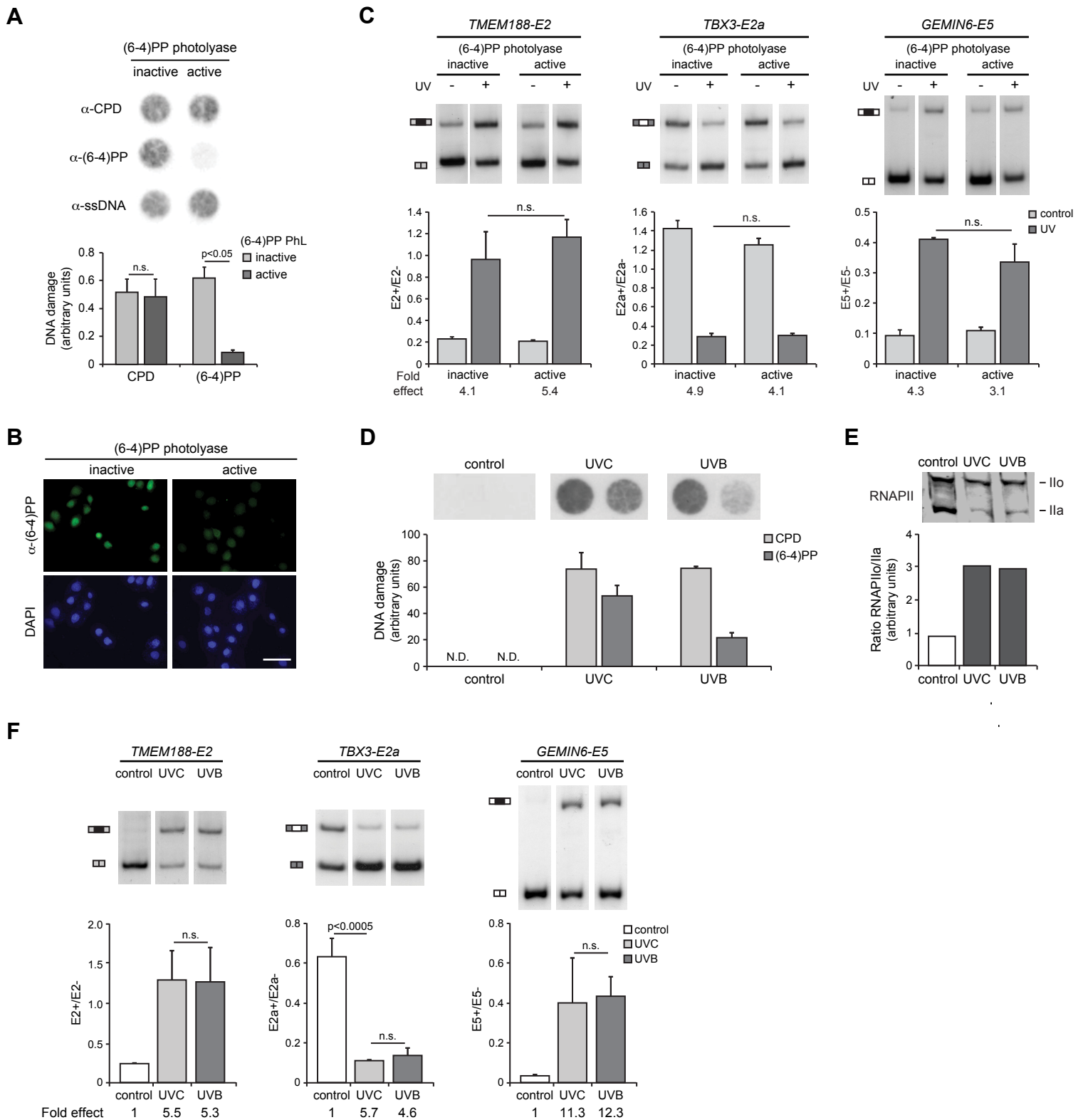


**Figure S2. Cyclobutane Pyrimidine Dimers Are Responsible for the UV Effect on AS, Related to Figure 1**

**(A)** DNA repair in HaCaT cells transduced with *Arabidopsis thaliana* (6-4)PP photolyase as described in Figure 1B was assessed by DNA western dot blot using specific antibodies against CPD, (6-4)PP or total single-stranded DNA (ssDNA). Experiments were performed in triplicates. Mean, SEM and p-values (Student's t-test) of a representative experiment are shown.

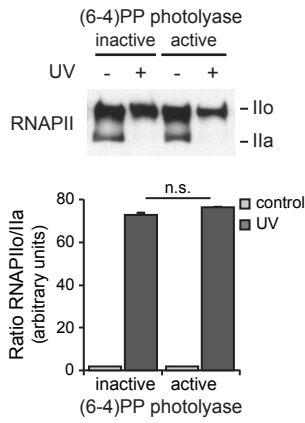
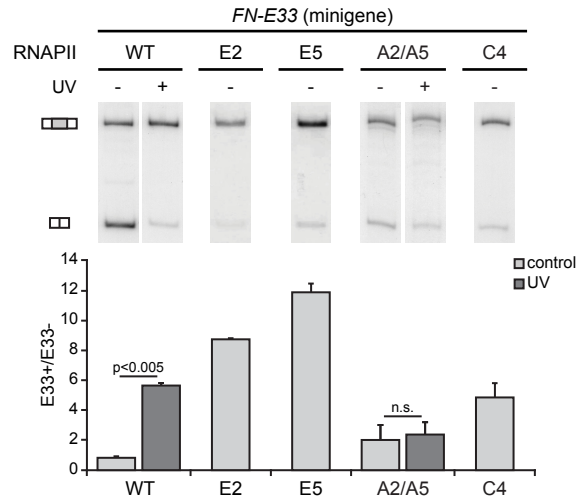
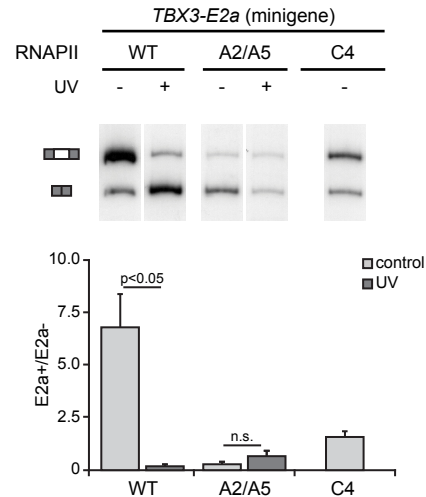
**(B)** (6-4)PP repair by (6-4)PP photolyase. HaCaT cells plated on coverslips were transduced with an adenovirus expressing the (6-4)PP photolyase. After 72 h, cells were irradiated with 15 J/m<sup>2</sup> and the photolyase was activated by exposure to white light for 2 h. Immediately following photoreactivation, cells were fixed and (6-4)PP levels were detected by immunofluorescence. Scale bar represents 20  $\mu$ m.

**(C)** HaCaT cells were transduced with (6-4)PP photolyase as in (A) and irradiated with 15 J/m<sup>2</sup> of UV, followed by photoactivation. After 6 h, cells were harvested and the AS of the indicated endogenous genes was assessed by radioactive RT-PCR. Experiments were performed in triplicates and mean, SEM and p-values (Student's t-test) of a representative experiment are shown.

**(D)** HaCaT cells were irradiated with UVC (15 J/m<sup>2</sup>) or UVB (3300 J/m<sup>2</sup>) to generate comparable levels of CPDs. Immediately after irradiation, cells were harvested. Genomic DNA was extracted and the levels of CPD and (6-4)PP photoproducts were detected by DNA western dot blot.

**(E)** RNAPII phosphorylation status in HaCaT cells irradiated as in (D) was analyzed as described, 2 h after treatment. The phospho RNAPII (Ilo) to non-phospho RNAPII (Ila) ratio of a representative experiment is shown.

**(F)** HaCaT cells were irradiated as in (D) and harvested after 6 h. AS of the indicated endogenous genes was assessed by radioactive RT-PCR.

**A****B****C**

**Figure S3. Cyclobutane Pyrimidine Dimers Modulate RNAPII Phosphorylation and Elongation Rates, Related to Figure 2**

**(A)** RNAPII phosphorylation status in (6-4)PP photolyase-transduced HaCaT cells treated with 15 J/m<sup>2</sup> of UV was assessed 2 h after photolyase activation. Global RNAPII phosphorylation pattern was determined by western blot and the phospho RNAPII (Ilo) to non-phospho RNAPII (Ila) ratio of a representative experiment is shown. Mean, SEM and p-values from two experiments are shown.

**(B-C)** RNAPII phosphorylation and elongation mediate the DNA damage effect on AS. HaCaT cells were transfected with expression plasmids encoding  $\alpha$ -amanitin-resistant wild type (WT) RNAPII large subunit (Rpb1) as well as different mutant versions in which serine residues at positions 2 and 5 were replaced by glutamic acid (E2, E5) or alanine (A2/A5) or a slow (C4) polymerase together with the *FN-E33* **(B)** or *TBX3-E2a* **(C)** reporter minigenes and treated as described (Muñoz *et al.*, 2009). Cells were irradiated with 15 J/m<sup>2</sup> of UV and 24 h later AS of *FN* or *TBX3* was assessed by radioactive RT-PCR with specific pairs of primers for the minigenes derived mRNAs. As can be seen, the usage of phosphomimetic polymerases (E2 and E5) duplicates the UV effect while the usage of the A2/A5 RNAPII, which cannot be phosphorylated, prevents the effect. Moreover, a slow RNAPII (C4) mimics the UV effect on AS. All experiments were performed in triplicates and mean and SEM of a representative experiments are shown.

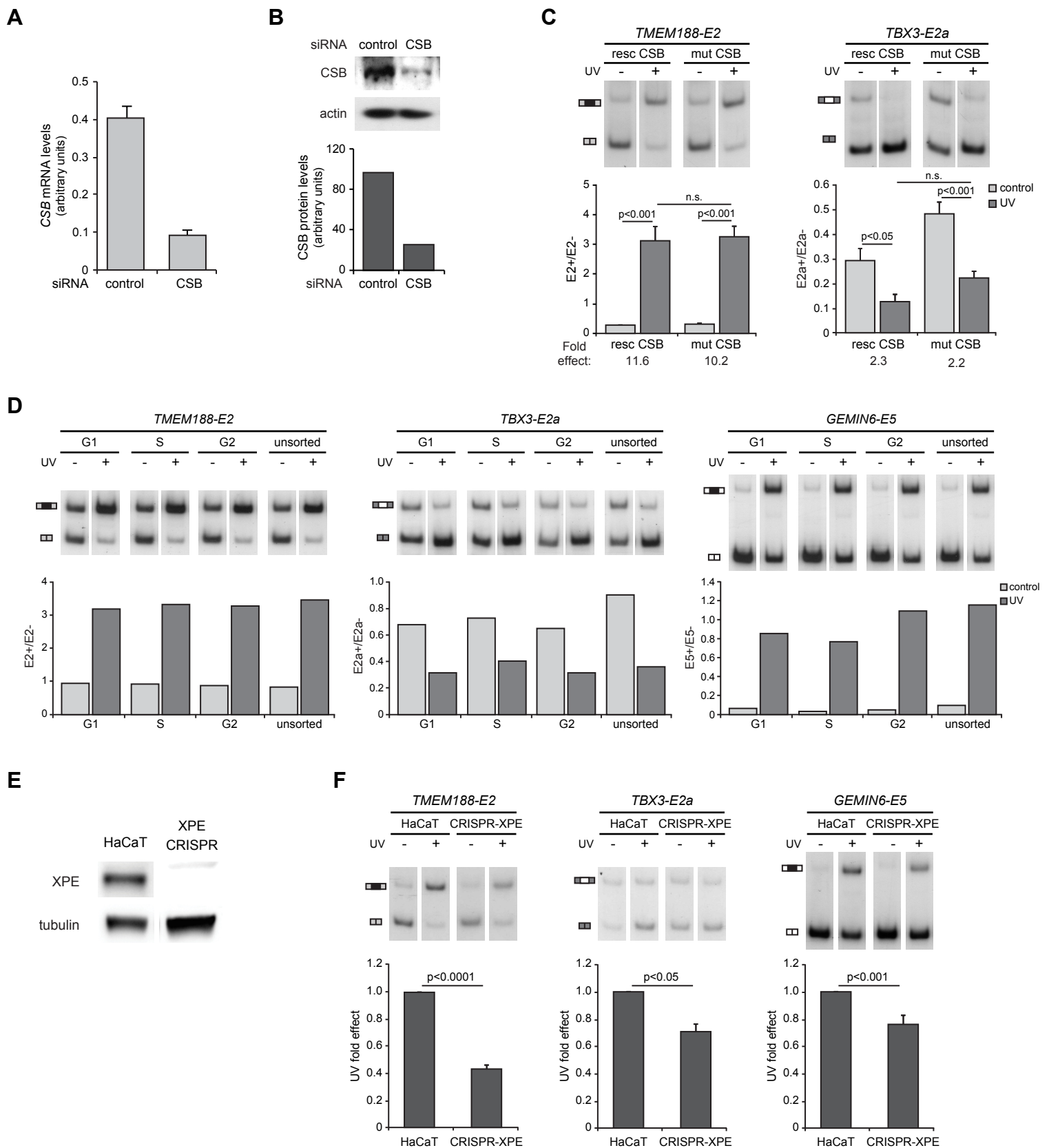


**Figure S4. AS Regulation by UV Is Not Affected by TC-NER Nor Cell Cycle Position but Requires GG-NER Factor XPE, Related to Figure 3**

(A-B) HaCaT cells were transfected with 25 nM of control or CSB siRNA oligonucleotides for 72 h. (A) CSB mRNA levels were assessed by RT-qPCR. mRNAs levels were normalized to housekeeping *HSPCB* mRNA levels. (B) CSB protein levels were detected by western blot. (C) Cells from CSB patients (CS1ANV CSB, “mut CSB”) or rescued by re-expression of the CSB protein (CS1ANSV HA CSB HIS, “resc CSB”) were UV irradiated ( $15 \text{ J/m}^2$ ) and harvested 6 h later. AS of the indicated endogenous genes was assessed by radioactive RT-PCR. The inclusion levels of *GEMIN6* in CSB cells, either mutated or rescued, was not detectable.

(D) HaCaT cells were stained and sorted according to their DNA content. RNA was extracted from G1, S, and G2 populations and AS of the indicated endogenous genes was assessed by radioactive RT-PCR.

(E) An XPE null keratinocyte clone was obtained from HaCaT cells using the CRISPR Cas-9 technology. XPE ablation was confirmed by western blot. The experiment involving the screening of multiple control and XPE-ablated clones, the figure shows two panels from non-adjacent lanes.

(F) Wild type cells (HaCaT) and XPE knockout cells (CRISPR-XPE) were irradiated with  $15 \text{ J/m}^2$  and harvested 6 h later. AS patterns were determined as described. Mean, SEM and p-values (Student’s t-test,  $n \geq 4$ ) are shown.

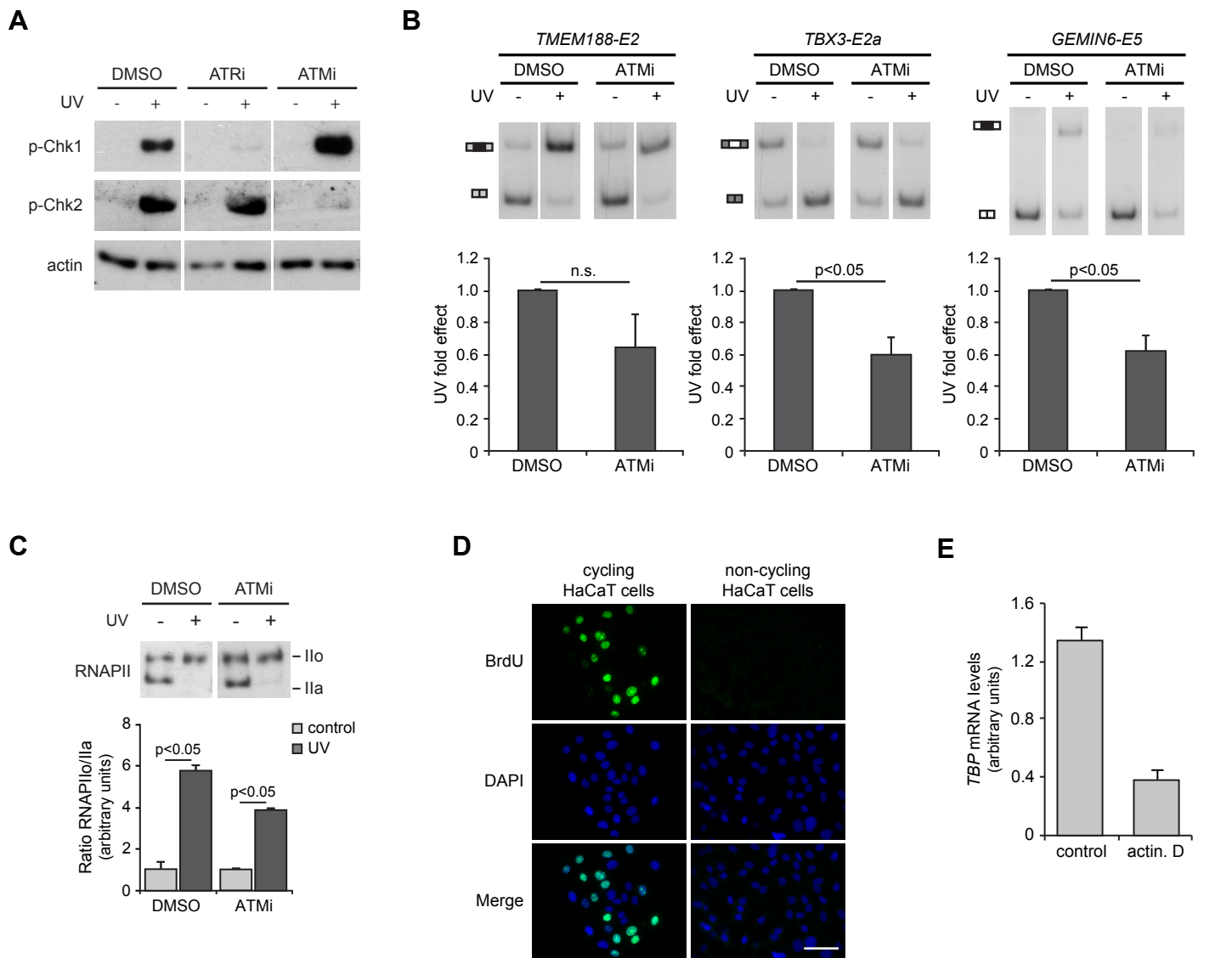


**Figure S5. Role of ATM in the Response to UV, Related to Figures 4 and 5**

**(A)** HaCaT cells were pre-treated with 10  $\mu$ M of ATR inhibitor (ATRi) or 10  $\mu$ M of ATM inhibitor (ATMi) for 1 h before UV irradiation. Cells were harvested 2 h later and phosphorylation levels of Chk1 and Chk2, the ATR and the ATM downstream targets, respectively, were assessed by western blot.

**(B)** HaCaT cells were pre-treated with 10  $\mu$ M of ATM inhibitor (ATMi) 1 h prior to UV irradiation (15 J/m<sup>2</sup>). After 6 h, AS of the indicated endogenous genes was assessed by radioactive RT-PCR. Images from a representative experiment and mean, SEM and p-values from three experiments are shown.

**(C)** RNAPII phosphorylation status in HaCaT cells pre-treated with ATMi was analyzed as described, 2 h after UV irradiation with 15 J/m<sup>2</sup>. Images from a representative experiment and mean, SEM and p-values from three experiments are shown.

**(D)** HaCaT cells grown in normal conditions ("cycling cells") or under a serum-deprivation protocol ("non cycling cells") were pulsed with 10  $\mu$ M BrdU for 1 h. Cells were fixed and BrdU incorporation was detected by immunofluorescence. Scale bar represents 20  $\mu$ m.

**(E)** Transcription inhibition by actinomycin D. HaCaT cells were treated with 5 ng/ $\mu$ l actinomycin D for 7 h and levels of short-lived *TBP* mRNA were assessed by RT-qPCR and normalized to levels of long-lived housekeeping *HSPCB* mRNA.

## Supplemental Information

### Supplemental Tables

#### Table S1 (Excel file). Related to Figure 1.

Genome wide analysis of UV modulated ASEs.

*Full coordinate: chromosome: C1 donor, AS exon, C2 acceptor. Strand is "+" if C1 donor coordinate is smaller than C2 acceptor coordinate, and "-" otherwise. Alt3/Alt5, alternative splice site acceptor/donor selection; IR, intron retention; AltEx, cassette alternative exons (including microexons when length  $\leq 27$  nt).*

#### Table S2 (Excel file). Related to Figure 1.

Gene ontology analysis of ASEs modulated by UV and reverted by CPD photolyase in categories cell cycle, apoptosis and DNA damage.

### Supplemental Experimental Procedures

#### Cell Culture and Treatments

Cells from CSB patients (CS1ANV CSB, "mut CSB") or rescued by re-expression of the CSB protein (CS1ANSV HA CSB HIS, "resc CSB"), originally described in Troelstra et al. (1992), were a generous gift from Frédéric Coin and Jean Marc Egly (Strasbourg, France).

When indicated, HaCaT cells were pre-incubated for 1 h before UV irradiation with ATM inhibitor 10  $\mu$ M (KU-60019, Abcam).

#### CPD and (6-4)PP Immunofluorescence

HaCaT cells grown on cover slips were transduced with adenoviruses expressing the CPD photolyase from *Potorous tridactylus* or the (6-4)PP photolyase from *Arabidopsis thaliana*. After 72 h, cells were irradiated with 15 J/m<sup>2</sup> and the photolyases were activated by exposure to white light for 2 h. Immediately following photoactivation, cover slips were washed with PBS, and cells were fixed in 4% paraformaldehyde for 15 min at 20°C. Cover slips were then stored at 4°C in PBS until processed. Cover slips were washed 2 times with PBS and DNA was denatured by treatment with 1 N HCl for 10 min. Following 3 washes with PBS, cover slips were then blocked for 1 h 30 min in 5% normal goat serum (NGS) in PBS at room temperature, washed with PBS and incubated with anti-CPD or anti-(6-4)PP antibodies (TDM-2 and 64M-2, Cosmo Bio; 1:250) in 5% NGS/PBS for 1 h at room temperature. After washing 3 times with PBS, cover slips were incubated for 30 min at room temperature with Alexa-conjugated anti-mouse antibody (Molecular Probes; 1:200) in 5% NGS/PBS, washed 3 times for 5 min in PBS and stained with DAPI (0.1 g/ml DAPI in PBS). After 2 washes with PBS, cover slips were finally mounted in 50% glycerol in PBS. Fluorescence was captured with an Olympus IX-81 microscope, using an HQ2 (Roper Scientific) cooled CCD camera and Metamorph software (Molecular Devices).

#### Global Transcriptome Analysis of Alternative Splicing

RNA prepared as described in Experimental Procedures was sequenced on an Illumina HiSeq2000 (producing between 98.1 to 113.8 million 125-nt paired end reads per sample). Transcriptome-wide AS and gene expression profiling was performed using our recently described pipeline (*vast-tools* (Irimia et al, 2014)), which provides accurate inclusion levels using exon-exon (or exon-intron) junction reads for all types of AS, including single and complex exon skipping events, microexons, alternative donor and acceptor choices and intron retention. For an ASE to be considered as differentially regulated between "no UV" and UV-treated samples, we required: (i) an average  $\Delta$ PSI between samples of at least 15%, and (ii) a  $\Delta$ PSI between the ranges of both samples of at least 5. These comparisons were performed using *vast-tools* compare with the following parameters: --min\_dPSI 15 --min\_range 5. Moreover, only ASEs with enough read coverage in all six samples were considered, according to the following criteria (modified from (Irimia et al, 2014):

- For cassette exons (except for those quantified using the microexon pipeline): (i)  $\geq 15$  reads mapping to the sum of exclusion EEJs, OR (ii)  $\geq 15$  reads mapping to one of the two inclusion EEJs, and  $\geq 10$  to the other inclusion EEJ.
  - For microexons: (i)  $\geq 15$  reads mapping to the sum of exclusion EEJs, OR (ii)  $\geq 15$  reads mapping to the sum of inclusion EEJs.
  - For IR: (i)  $\geq 15$  reads mapping to the sum of skipping EEJs, OR (ii)  $\geq 15$  reads mapping to one of the two inclusion EEJs, and  $\geq 10$  to the other inclusion EEJ. In addition, IR events with a significant imbalance between reads mapping at both EEJs (as assessed by a binomial test, (Braunschweig et al, 2014)) in any of the samples were discarded.
  - For Alt3 and Alt5:  $\geq 15$  reads mapping to the sum of all EEJs involved in the specific event.
- Gene expression levels are measured using the cRPKM metric (Labbe et al, 2012).

### UBV Irradiation

UVB irradiation was performed with an XX-15M UVB bench lamp (UVP) in combination with a 65CGA-305 glass filter (Newport) that filters light below 307 nm. The dose was quantified with a UVX Radiometer (UVP).

### Transfection of RNAPII Mutants

Transfection of expression plasmids and AS reporter minigenes was performed using Lipofectamine 2000 (Thermo) according to manufacturer's instructions.

Conditions for expression of  $\alpha$ -amanitin-resistant variants of the largest subunit of human RNAPII (hRPB1) were previously described (de la Mata et al, 2003; Muñoz et al, 2009).

### RNA Extraction and Radioactive RT-PCR Analysis

RNA was purified using TriPure reagent (Roche Life Science). Conditions and primers for radioactive reverse-transcriptase polymerase chain reaction (RT-PCR) of endogenous or reporter minigenes are as follows:

Radioactive RT-PCR Analysis:

Primer sequences:

<i>FN-E33</i> (minigene)	F: 5' CACTGCCTGCTGGTGACTCGA 3' R: 5' GCGGCCAGGGGTCACGAT 3'
<i>FN-E33</i> (endogenous)	F: 5' AGCCCCGCAAGCAGCAAGCC 3' R: 5' GTAGCATCTGTACACGAG 3'
<i>GEMIN6</i> (endogenous)	F: 5' CTACAGACCCAGTCTCTGCCA 3' R: 5' CTCCCTGTTCAGTGATGGGGA 3'
<i>TBX3-E2a</i> (minigene)	F: 5' TTCAAGCTCCTAAGCCACTG 3' R: 5' GGGCTGGTATTTGTGCATGGA 3'
<i>TBX3-E2a</i> (endogenous)	F: 5' ATGTACATTCACCCGGACAGC 3' R: 5' GGGCTGGTATTTGTGCATGGA 3'
<i>TMEM188</i> (endogenous)	F: 5' GAAGCTGCGATGCGGACAG 3' R: 5' TTCTCCAGCGTCCAGTAGCAG 3'
<i>CCNL1</i> (endogenous)	F: 5' TGCATCAAAAATCGAAGAAGCACC 3' R: 5' TCCCAACTCCTTTAGCACCCCT 3'
<i>IL17RA</i> (endogenous)	F: 5' GCCTCAATGACTGCCTCAGAC 3' R: 5' CGGTGTATTTGGTGTTCATCACTG 3'
<i>RASSF7</i> (endogenous)	F: 5' AACCTGCAGCAGTTCATCCAG 3' R: 5' CCCTCACTAGGCTGTACAGA 3'
<i>SFRS17A</i> (endogenous)	F: 5' GCCGGAATCAGAAGAAGCTGG 3' R: 5' TCCTGTTCCCGTAGCTTCACA 3'

PCR Conditions:

	Reaction conditions	PCR Program
<i>FN-E33</i>	[Mg <sup>2+</sup> ] = 1,5 mM	94°C x 2 min, 31 cycles of: [94°C x 1 min,

(minigene)	[DMSO] = 3%	56°C x 1 min, 72°C x 1 min]
<i>FN-E33</i> (endogenous)	[Mg <sup>2+</sup> ] = 1,5 mM [DMSO] = 3%	94°C x 2 min, 30 cycles of: [94°C x 1 min, 62°C x 1 min, 72°C x 2 min], 72°C x 10 min
<i>GEMIN6</i> (endogenous)	[Mg <sup>2+</sup> ] = 3 mM [DMSO] = 5%	94°C x 2 min, 30 cycles of: [94°C x 20 sec, 63°C x 20 sec, 72°C x 20 sec]
<i>TBX3-E2a</i> (minigene)	[Mg <sup>2+</sup> ] = 2 mM	94°C x 2 min, 30 cycles of: [94°C x 20 sec, 60°C x 20 sec, 72°C x 20 sec], 72°C x 1 min
<i>TBX3-E2a</i> (endogenous)	[Mg <sup>2+</sup> ] = 4 mM	94°C x 2 min, 30 cycles of: [94°C x 20 sec, 63°C x 20 sec, 72°C x 20 sec]
<i>TMEM188</i> (endogenous)	[Mg <sup>2+</sup> ] = 1,5 mM [DMSO] = 3%	94°C x 2 min, 30 cycles of: [94°C x 20 sec, 60°C x 20 sec, 72°C x 20 sec]
<i>CCNLI</i> (endogenous)	[Mg <sup>2+</sup> ] = 1,5 mM [DMSO] = 5%	94°C x 2 min, 30 cycles of: [94°C x 20 sec, 60°C x 20 sec, 72°C x 20 sec]
<i>IL17RA</i> (endogenous)	[Mg <sup>2+</sup> ] = 3 mM	94°C x 2 min, 30 cycles of: [94°C x 20 sec, 63°C x 20 sec, 72°C x 20 sec]
<i>RASSF7</i> (endogenous)	[Mg <sup>2+</sup> ] = 1,5 mM [DMSO] = 5%	94°C x 2 min, 30 cycles of: [94°C x 20 sec, 63°C x 20 sec, 72°C x 20 sec]
<i>SFRS17A</i> (endogenous)	[Mg <sup>2+</sup> ] = 1,5 mM [DMSO] = 5%	94°C x 2 min, 30 cycles of: [94°C x 20 sec, 63°C x 20 sec, 72°C x 20 sec]

### Quantitative Real-Time PCR

cDNAs were amplified using Taq DNA polymerase (Invitrogen) with SYBR green using an Eppendorf Mastercycler. Primers and PCR conditions for CSB, HSPCB and TBP were as follows:

Primer sequences:

<i>CSB</i>	F: 5' GCGGCGGTAGCGTCTCTG 3' R: 5' ACCACCACTTTCTTGCTTGATTGC 3'
<i>HSPCB</i>	F: 5' CCAAAAAGCACCTGGAGATCA 3' R: 5' TGTCGGCCTCAGCCTTCT 3'
<i>TBP</i>	F: 5' AGACCATTGCACTTCGTGCC 3' R: 5' AAATCAGTGCCGTGGTTCGT 3'

PCR conditions:

	Reaction conditions	PCR Program
<i>CSB, HSPCB</i>	[Mg <sup>2+</sup> ] = 4 mM	94°C x 2 min, 40 cycles of: [94°C x 20 sec, 64°C x 20 sec, 72°C x 20 sec]
<i>TBP</i>	[Mg <sup>2+</sup> ] = 4 mM	95°C x 2 min, 40 cycles of: [95°C x 15 sec, 60°C x 15 sec, 72°C x 20 sec]

Data was analyzed with Realplex software using the relative standard curve method and normalized to housekeeping HSPCB mRNA levels. Reactions were performed in duplicates or triplicates.

### Cell Sorting

Live HaCaT cells were stained with Violet Vybrant Dye (Life Technologies) in order to sort cells according to their DNA content. Violet 405 nm excitation was used with a 440/40 nm bandpass filter according to the manufacturer's instructions with minor modifications. G1, S and G2/M populations were sorted and alternative splicing was analyzed as described.

### Bromodeoxyuridine Incorporation

HaCaT cells were plated on coverslips and grown as described. For non-cycling cells, HaCaT cells were grown to confluence and further incubated for 3 days in low serum (0.5% FBS) medium. Cells were then pulsed with Bromodeoxyuridine (BrdU) that was added to the culture medium at a final 10 µM concentration for 1 hour. Cells were then washed with PBS and fixed in cold methanol for 20 min at -20°C,

followed by cold acetone for 40 seconds. Cover slips were washed 3 times with PBS and DNA was denatured by treatment with 1 N HCl for 15 min at room temperature. Following 3 washes with PBS, cells were permeabilized with 0.1% Triton-X in PBS for 15 minutes at 4°C. Cover slips were then blocked overnight in 5% bovine serum albumin (BSA) in PBS at 4°C and incubated with anti-BrdU antibody (Medical and Biological Laboratories Co., #MI-11-3; 1:100) in 5% BSA in PBS for 1 h at room temperature. After washing 3 times with PBS-0.05% Tween for 10 min, cover slips were incubated for 1 hour at room temperature with Alexa 488-conjugated anti-mouse antibody (Molecular Probes; 1:100) in 5% BSA in PBS, washed once for 15 min in PBS-0.05% Tween and stained with DAPI (0.1 g/ml DAPI in PBS-0.05% Tween). After one wash with PBS, cover slips were mounted in Vectashield (Vector Laboratories Inc.) Fluorescence was captured with an Olympus IX-81 microscope, using an HQ2 (Roper Scientific) cooled CCD camera and Metamorph software (Molecular Devices).

#### **HaCaT XPE Knockout Cell Line (CRISPR-Cas9)**

For the construction of the HaCaT XPE KO clone we followed the protocol described in (Ran et al., 2013). The guide RNA for Cas9 targets the first coding exon of *XPE* genomic locus and was designed using the CRISPR design tool (<http://tools.genome-engineering.org>). The guide was obtained by annealing the following primer pair 5'-CACCGGGGCGTAATACAATCTCGG- 3'; 5'-AAACCCGAGATTGTATTA CGCCCC- 3' and was cloned into the pSpCas9(BB)-2A-puro (PX459) vector digested with the restriction enzyme BbsI. Stable transfectants were selected with Puromycin and single clones were isolated by clonal-density dilution. XPE protein levels were assayed by western blot.

#### **Western Blot**

Proteins were electrophoresed in SDS-polyacrylamide gel electrophoresis, transferred to nitrocellulose membranes (Bio-Rad) and blotted with antibodies against RNAPII (N-20, sc-899, Santa Cruz), CSB (clones 3H8 and 1A11, a gift from J.M.Egly and Frédéric Coin), p-Chk1 Ser317 (#2344, Cell Signaling), p-Chk2 Thr68 (#2661, Cell Signaling) and  $\beta$ -actin (sc-47778, Santa Cruz).

#### **Supplemental References**

Braunschweig U, Barbosa-Morais NL, Pan Q, Nachman EN, Alipanahi B, Gonatopoulos-Pournatzis T, Frey B, Irimia M, Blencowe BJ (2014) Widespread intron retention in mammals functionally tunes transcriptomes. *Genome Res* 24: 1774-1786

Irimia M, Weatheritt RJ, Ellis JD, Parikshak NN, Gonatopoulos-Pournatzis T, Babor M, Quesnel-Vallieres M, Tapial J, Raj B, O'Hanlon D, Barrios-Rodiles M, Sternberg MJ, Cordes SP, Roth FP, Wrana JL, Geschwind DH, Blencowe BJ (2014) A highly conserved program of neuronal microexons is misregulated in autistic brains. *Cell* 159: 1511-1523

Labbe RM, Irimia M, Currie KW, Lin A, Zhu SJ, Brown DD, Ross EJ, Voisin V, Bader GD, Blencowe BJ, Pearson BJ (2012) A comparative transcriptomic analysis reveals conserved features of stem cell pluripotency in planarians and mammals. *Stem Cells* 30: 1734-1745

Muñoz M, Pérez Santangelo M, Paronetto M, de la Mata M, Pelisch F, Boireau S, Glover-Cutter K, Bendov C, Blaustein M, Lozano J, Bird G, Bentley D, Bertrand E, Kornblihtt A (2009) DNA damage regulates alternative splicing through inhibition of RNA polymerase II elongation. *Cell* 137: 708-720

Ran FA, Hsu PD, Wright J, Agarwala V, Scott DA, Zhang D (2013) Genome engineering using the CRISPR-Cas9 system. *Nat Protoc* 8, 2281–2308

Troelstra C, van Gool A, de Wit J, Vermeulen W, Bootsma D, Hoeijmakers JH (1992) ERCC6, a member of a subfamily of putative helicases, is involved in Cockayne's syndrome and preferential repair of active genes. *Cell* 71: 939-953